Molecular Microbiology (2017) 00(00), 00–00

doi:10.1111/mmi.13744
First published online 2017

MybA, a transcription factor involved in conidiation and conidial viability of the human pathogen *Aspergillus fumigatus*

Isabel Valsecchi,[1†] Özlem Sarikaya-Bayram,[2†] Joanne Wong Sak Hoi,[1†‡] Laetitia Muszkieta,[1†] John Gibbons,[3§] Marie-Christine Prevost,[4] Adeline Mallet,[4] Jacomina Krijnse-Locker,[4] Oumaima Ibrahim-Granet,[5] Isabelle Mouyna,[1] Paul Carr,[6] Michael Bromley,[6] Vishukumar Aimanianda,[1] Jae-Hyuk Yu,[7] Antonis Rokas,[3] Gerhard H Braus,[8] Cosmin Saveanu,[9] Özgür Bayram[2,8¶] and Jean Paul Latgé [1*]**

[1]*Unité des Aspergillus, Institut Pasteur, Paris 75015, France.*
[2]*Department of Biology, Maynooth University, Maynooth, Co. Kildare, Ireland.*
[3]*Department of Biological Sciences, Vanderbilt University, Nashville, TN 37235, USA.*
[4]*Plate-Forme de Microscopie Ultrastructurale, Institut Pasteur, Paris 75015, France.*
[5]*Unité de Recherche Cytokines & Inflammation Institut Pasteur, Paris 75015, France.*
[6]*Manchester Fungal Infection Group, Institute of Inflammation and Repair, University of Manchester, Manchester, UK.*
[7]*Department of Bacteriology and Genetics, University of Wisconsin, Madison, WI 53706, USA.*
[8]*Department of Molecular Microbiology and Genetics, Georg August University, Göttingen 37077, Germany.*
[9]*Unité de Génétique des Interactions Macromoléculaires, CNRS UMR3525, Institut Pasteur, Paris, France.*

Summary

***Aspergillus fumigatus*, a ubiquitous human fungal pathogen, produces asexual spores (conidia), which are the main mode of propagation, survival and infection of this human pathogen. In this study, we present the molecular characterization of a novel regulator of conidiogenesis and conidial survival called MybA because the predicted protein contains a Myb DNA binding motif. Cellular localization of the MybA::Gfp fusion and immunoprecipitation of the MybA::Gfp or MybA::3xHa protein showed that MybA is localized to the nucleus. RNA sequencing data and a *uidA* reporter assay indicated that the MybA protein functions upstream of *wetA*, *vosA* and *velB*, the key regulators involved in conidial maturation. The deletion of *mybA* resulted in a very significant reduction in the number and viability of conidia. As a consequence, the Δ*mybA* strain has a reduced virulence in an experimental murine model of aspergillosis. RNA-sequencing and biochemical studies of the Δ*mybA* strain suggested that MybA protein controls the expression of enzymes involved in trehalose biosynthesis as well as other cell wall and membrane-associated proteins and ROS scavenging enzymes. In summary, MybA protein is a new key regulator of conidiogenesis and conidial maturation and survival, and plays a crucial role in propagation and virulence of *A. fumigatus*.**

Introduction

Aspergillus fumigatus is a ubiquitous saprotrophic ascomycete that plays an important role in recycling the carbon and nitrogen in nature. Asexual spores (conidia), produced abundantly in the natural habitats of this filamentous fungus, are responsible for the dispersal of this fungus. These conidia are quiescent and can remain dormant for more than a year (Lamarre *et al.*, 2008). These metabolically inert conidia will only germinate under favorable nutritional conditions. This capacity

Accepted 4 July, 2017. For correspondences. *E-mail jean-paul.latge@pasteur.fr; Tel. +33-140613518; Fax +33-140613419 or **E-mail ozgur.bayram@nuim.ie; Tel. +35317086879 †These authors contributed equally to this work. Present addresses: ‡Institute of Biomedical Research, Novartis, Basel, Switzerland §Department of Biology, Clark University, Worcester, MA, 01610, USA ¶Department of Biology, National University of Ireland Maynooth, Maynooth, Co. Kildare, Ireland

allows conidia to find an environment where *A. fumigatus* can establish itself and thrive, which consequently ensure its survival and propagation in nature. Airborne conidia entering the human lung can reach different levels of the respiratory tract, up to alveoli owing their small size, and upon finding a favorable nutritional environment they start germination. Conidial germination leads to the establishment of pulmonary aspergillosis, the severity of which will depend on the immune status of the host. In spite of its importance, the molecular mechanisms underlying entry and exit pathways of conidial dormancy remain largely unknown.

In contrast, the asexual development (conidiation) of *Aspergillus* has been extensively studied. Under starvation, hyphae differentiate into thick-walled foot cells and produce aerial stalk initials. A multi-nucleated vesicle forms by swelling of the stalk apex. A layer of phialides is formed on the surface of the vesicle and a single nucleus enters each cell. Following asymmetric mitotic divisions of the phialide nuclei, conidia bud off from the tip of the phialide to form chains of clonally derived spores (Yu, 2010). Conidiation is a precisely and genetically programmed event responding to external signals. The central regulatory pathway (BrlA(AFUA_1G16590) → AbaA(AFUA_1G04830) → WetA(AFUA_4G13230)) governs conidiation in *A. fumigatus* and controls the expression of conidiation specific genes during conidiophore formation and conidial maturation (Mah and Yu, 2006; Tao and Yu, 2011). The Δ*brlA* mutant develops abnormal conidiophores that are unable to differentiate further (Tao and Yu, 2011). The Δ*abaA* loss-of-function mutants form defective conidiophores exhibiting elongated phialides that fail to generate conidia (Tao and Yu, 2011). The Δ*wetA* mutant produces colorless conidia that fail to separate from each other (Tao and Yu, 2011). More recently, the velvet family proteins VeA(AFUA_1G12490), VosA(AFUA_4G10860), VelB (AFUA_1G01970) and VelC (AFUA_4G09770) which share a DNA binding and dimerization domain reminiscent of NF-κB (Ahmed *et al*., 2013), have also been shown to be involved in the control of conidiation, and conidium maturation, although the interactions among all these regulators in *A. fumigatus* are not well understood (Bayram *et al*., 2010; Tao and Yu, 2011; Dhingra *et al*., 2012; Park *et al*., 2012a, 2012b, Bayram and Braus, 2012).

The velvet family proteins have been shown to be involved in the regulation of conidiation by light. In the darkness, after entry into the nucleus, the VeA/VelB complex associates with a methyltransferase LaeA(AFUA_1G14660) and the VelB/VeA/LaeA trimeric complex controls sexual development and secondary metabolism in *Aspergillus nidulans* (Bayram *et al*., 2008). The association of LaeA with the dimeric complex VosA-VelB complex links the secondary metabolism to the development. The VelB-VosA heterodimer becomes undetectable as soon as the fungus is transferred to the light. Accordingly, light represses asexual spore formation. Conidiation has been especially analyzed in two species of *Aspergillus*, *A. nidulans* and *A. fumigatus*, which display a similar life cycle. Although the same orthologous regulatory proteins have been identified, the models for the regulation of the conidiation in these two species are not completely identical (Park *et al*., 2012a, 2012b).

During a transcript profiling study aiming at identifying novel regulators of conidial development in *A. fumigatus*, we retrieved a gene encoding a putative Myb transcription factor, AFUA_3G07070 designated as MybA (Lamarre *et al*., 2008). In this work, we show that *A. fumigatus* MybA is a newly identified regulator which is involved in the control of conidial formation and maturation in *A. fumigatus* and plays an essential role in the survival of the conidia.

Results

mybA *(AFUA_3G07070) encodes an* Aspergillus *specific Myb-type transcription factor*

The putative transcription factor encoded by the gene AFUA_3G07070, which was identified earlier during a transcriptome analysis of early conidial germination (Lamarre *et al*., 2008), was present in the list of putative transcription factors identified *in silico* in *A. fumigatus* and reported at the Fungal Transcription Factor Database (ftfd.snu.ac.kr). Orthologous genes were found in many Ascomycetous species but were absent in the genomes of genera closely related to *Aspergillus* such as *Magnaporthe*, *Fusarium*, *Trichoderma* and *Verticillium* species and in all Basidiomycetes and Zygomycetes (Supporting Information Fig. S1). The gene was composed of 3166 bp, with four exons and three introns, and encoded a 911 amino acid protein. The Ensembl-Fungi program detected a putative Myb-type helix-turn-helix DNA binding domain in the C-terminal portion (positions 812–878), and hence this gene was named, *mybA*. Nuclear localization signals (NLS) were predicted by P-Sort between positions 701 and 749 (PPASRKR and RKRQEKAELQRKKRQRV). Expression of a functional Gfp fusion of the protein driven by the native promoter (Supporting Information Fig. S2) showed that this protein was located as defined spots in the nuclei of mycelium, conidiophores and resting conidia (nuclei and nuclear pores were labeled with Histone 2A::mRfp and Pom152::mRfp respectively in Fig.1). Pull-down experiments using 3xHa- or Gfp-tagged proteins to find MybA interacting proteins showed that importin α and β of *A. fumigatus* (AFUA_2G16090 and AFUA_1G15720) and a

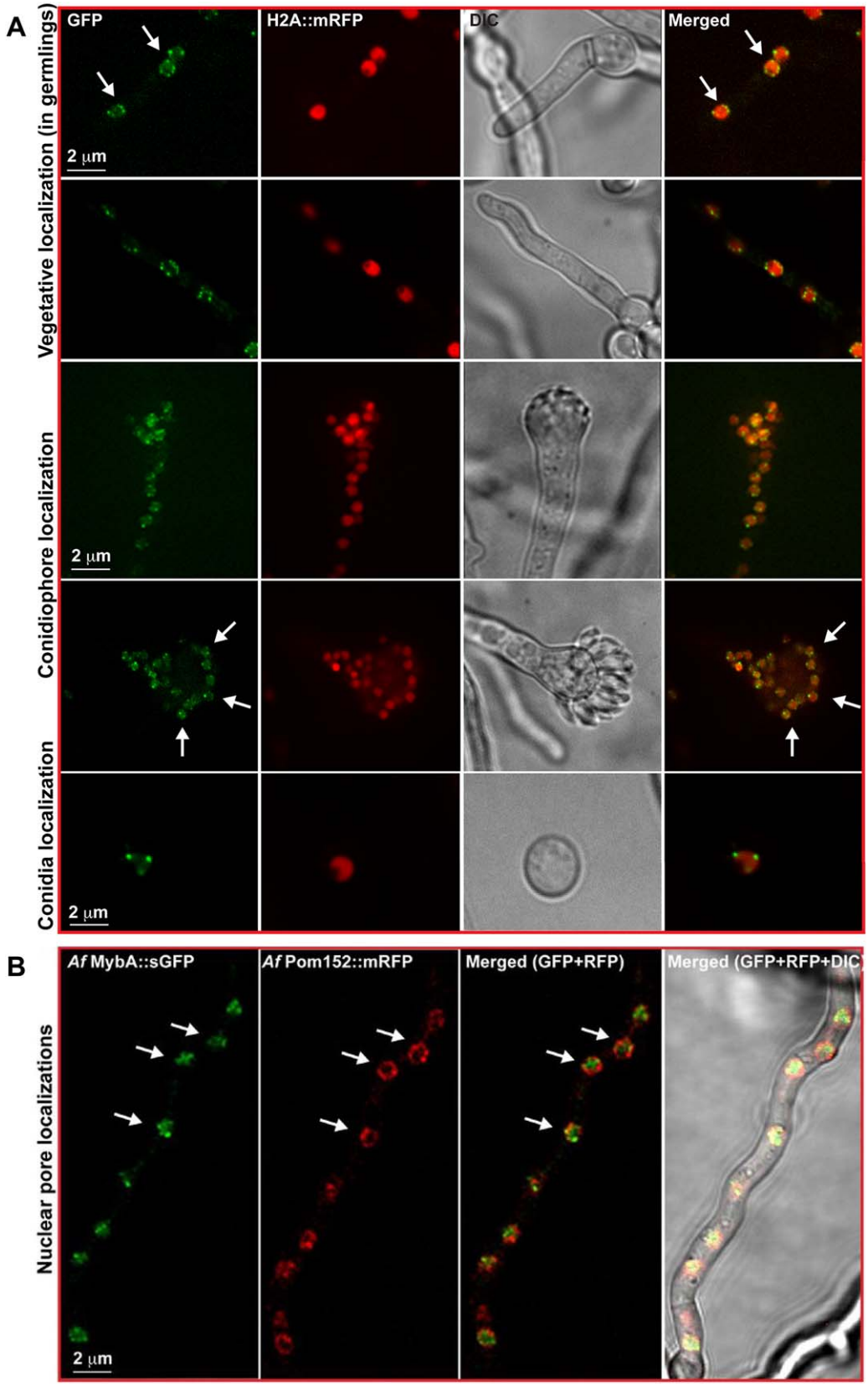

Fig. 1. Cellular localization of MybA::sGfp fusion during vegetative growth, conidiophore formation and conidia.
A. Cellular localization of the Af MybA::Gfp in vegetative and asexual stages of fungal development. Spots-like scattered nuclear localization of the Af MybA::sGfp strain was verified by the colocalization of the Histone 2A fused to monomeric red fluorescent protein (H2A::mRfp).
B. MybA partially localizes with nuclear pore complex Pom152::mRfp in vegetative cells. White arrows indicate the position of the nuclei in vegetative cells and conidiophores.

putative dynamin GTPase (AFUA_6G11890) were co-precipitated with MybA. This result confirmed an association of MybA with the nucleus and nuclear proteins (Fig. 2). The *in silico* data and the nuclear localization results were all in agreement with a putative function of this protein as a nuclear transcription factor.

The conidiation and conidial viability are affected in the ΔmybA *mutant*

To gain insight into the role of MybA, the Δ*mybA* mutant and the complemented Δ*mybA* strains were constructed in the CEA17_Δ*akuB*^{KU80} parental strain background (Supporting Information Fig. S3). On solid 2% malt or MM with 1% glucose media at 37°C, the mycelial growth

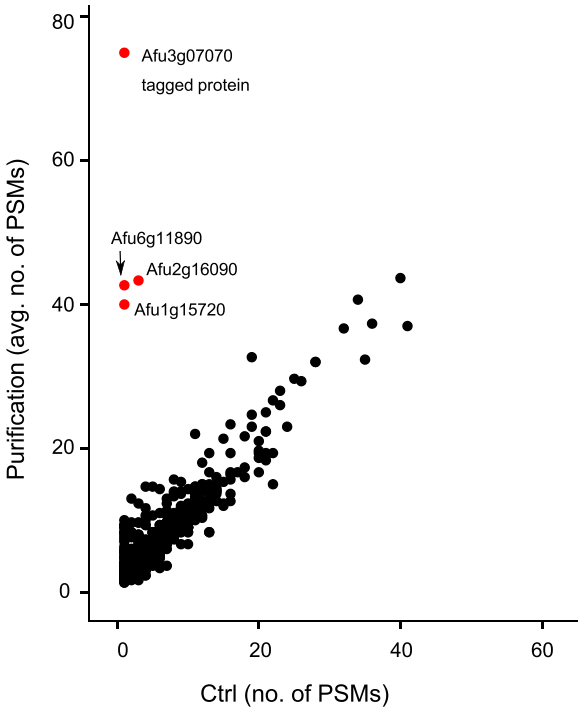

Fig. 2. Specific enrichment of proteins in association with Ha and Gfp tagged MybA as estimated from the average number of peptide spectra matches (PSM).
PSMs include all spectra leading to identification of a peptide for a given protein, even if several spectra correspond to the same peptide for three-independent purification replicates. The protein that are present to similar levels both in the control and in the purified sample show similar numbers of PSMs (the diagonal region of the scatterplot). Proteins that are specifically enriched are found in the upper left part of the graph. Proteins enriched in a similar experiment using Gfp- and Ha-tagged MybA are marked as red dots.

of the Δ*mybA* mutant appeared similar to the parental strain and the colony diameter was not significantly different between the parental and mutant strains (Fig. 3A and data not shown). Interestingly in liquid or agar-MM medium with low glucose concentration the mutant produce more mycelium than the parental strain at 37°C (Supporting Information Fig. S4).

In contrast, deletion of *mybA* affected conidiation (Fig. 3A and B) and altered conidial hydrophobicity (Supporting Information Fig. S5). The Δ*mybA* mutant produced about 40 times less conidium than the parental strains (Fig. 3B). Under light microscopy, conidiophores of the Δ*mybA* mutant looked almost devoid of conidia (Fig. 3A). The conidiation defects did not change upon prolonged cultivation (data not shown), indicating that the poor production of conidia was not due to a delayed progression of conidiation, as was observed in the Δ*flb* mutants (Wieser and Adams, 1995; Xiao *et al*., 2010). The conidiation defect was not rescued by KCl supplementation. Conidiation was similar when cultures were grown in darkness or exposed to day light (data not shown). In contrast to Δ*velB*, Δ*veA* and Δ*velC* mutants which conidiated in a 2% glucose with 1% peptone liquid medium in shaken flasks after 24 h of cultivation and to the Δ*vosA* mutant which produces conidiophores but not conidia under the same conditions (Park *et al*., 2012a, 2012b), the Δ*mybA* strain behaved in liquid culture like the parental strain and unlike Δ*velB*, Δ*veA*, Δ*velC* and Δ*vosA* mutants, did not produce any conidia or conidiophore. The conidiation defect was exacerbated with temperature: at 50°C the culture of the Δ*mybA* was totally sterile whereas the conidiation of the parental strain was not affected at this temperature (Fig. 3C).

Although conidiation was strongly reduced in the Δ*mybA* mutant, scanning and transmission electron microscopy studies showed that the Δ*mybA* mutant produced conidia which looked morphologically similar to the parental strain (Supporting Information Fig. S6). Conidia were echinulated with a dense and typical melanin outer layer in both parental and mutant strains. Moreover, the germination capacity of the conidia produced on Malt-agar media at room temperature was not affected and the germination kinetics of Δ*mybA* and parental conidia were similar on Sabouraud-agar medium (Supporting Information Fig. S7).

In contrast to germination, the Δ*mybA* mutant resting conidial survival in water was affected. The cell wall defect was not rescued by the addition of

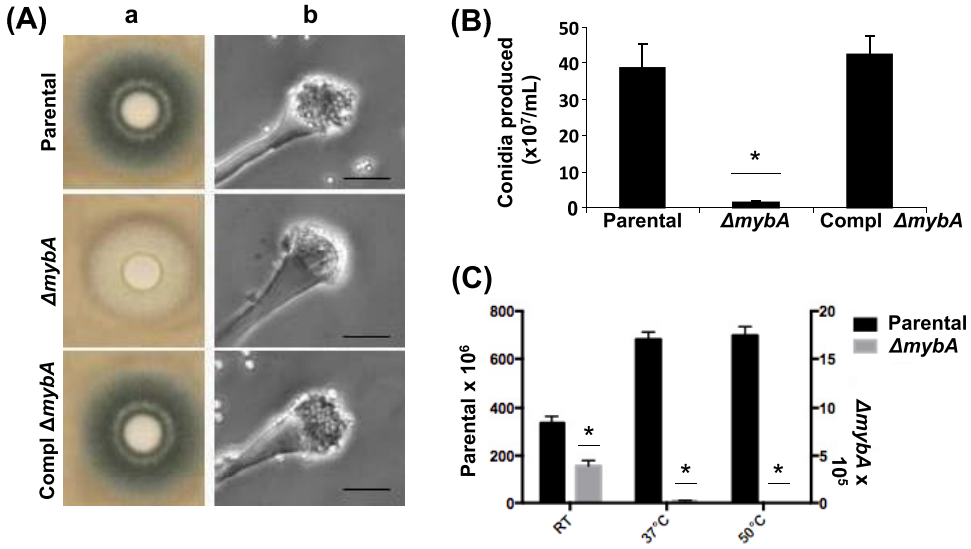

Fig. 3. Role of MybA in conidiation.
A. The phenotype of parental (CEA17_Δ*akuB*^{KU80}), Δ*mybA* and complemented Δ*mybA* (Compl Δ*mybA*) strains were compared. (a) Colonies grown on solid Sabouraud medium for 30 h at 37°C. (b) Microscopic examination of 7-day-old conidiophores obtained on solid 2% malt extract at 25°C.
B. Estimation of the conidia produced by the Δ*mybA* strain after 7 days of growth at 25°C on 2% malt agar slants inoculated with 10^5 conidia. Results are representative of three-independent experiments ± standard error.
C. Influence of the temperature on the conidiation of Δ*mybA* and parental strains. Note that the highest conidiation was found at 50°C for the parental strain whereas the Δ*mybA* strain was sterile at this temperature.

osmoprotectants into the culture medium (data not shown). When incubated in water at room temperature, the conidia of the Δ*mybA* mutant lost their viability in a few days with >90% of the conidia dying after 7 days of storage in water, whereas the conidia of the parental strain remained almost unaffected (Fig. 4A). After storing the conidia of the Δ*mybA* mutant for 2 days in water at 20°C, FITC could enter conidia of the Δ*mybA* mutant intracellularly indicating that the permeability of the conidia to external water-soluble molecules was affected (Fig. 4B). In contrast, no difference was observed in the viability of conidia of parental and mutant strains stored in water at 4°C over a period of up to 4 weeks or stored in the air at room temperature on the surface of a Malt agar medium (Supporting Information Fig. S8).

These data propose that *mybA* is required for production and viability of the conidia produced by *A. fumigatus*.

MybA is involved in the regulation of asexual sporulation but is not part of the central conidiation pathway

The transcript level of *mybA* throughout the life cycle of *A. fumigatus* was examined by real-time PCR. *mybA* transcripts were detected mainly in resting conidia and during late stages of development, when conidiation took place. In contrast, expression of *mybA* was low during germination (Fig. 5A and B). Since MybA was associated with conidiation, its position was assessed among the other regulators of asexual sporulation in *A. fumigatus*, which are *abaA*, *brlA*, *wetA*, *veA*, *vosA*, *velB* and *velC*. To reach this objective, an RNA-sequencing experiment was undertaken to compare 1-week-old conidiating cultures of the parental and Δ*mybA* mutant strains (Supporting Information Table S1). We used GFOLD to quantify gene expression (RPKM) and to identify differentially expressed genes based on the posterior distribution of expression log fold change (Feng *et al.*, 2012). GFOLD values less than −1 and greater than 1 were considered significantly downregulated and upregulated in the Δ*mybA* mutant respectively. We identified 1178 and 533 downregulated and upregulated genes respectively. Importantly, *mybA* was the most differentially expressed gene in the genome (GFOLD = −5.84929), and essentially absent in Δ*mybA* (RPKM = 0.137) while expressed at a high level in the parental strain (RPKM = 30.615). The RNA-seq data showed that *mybA* was controlling some transcription factors governing *A. fumigatus* conidiation. A strong down regulation of the expression of *wetA*, *vosA* and *velB* genes was observed in the Δ*mybA* strain with GFOLD values (Δ*mybA*/parental) respectively of −2.89, −1.99 and −1.68. The RNA seq analysis also showed that there was not any down regulation of the other transcription factors associated with conidiation (*abaA*, *brlA*, *stuA* (AFUA_2G07900), *medA* (AFUA_2G13260), *veA*,

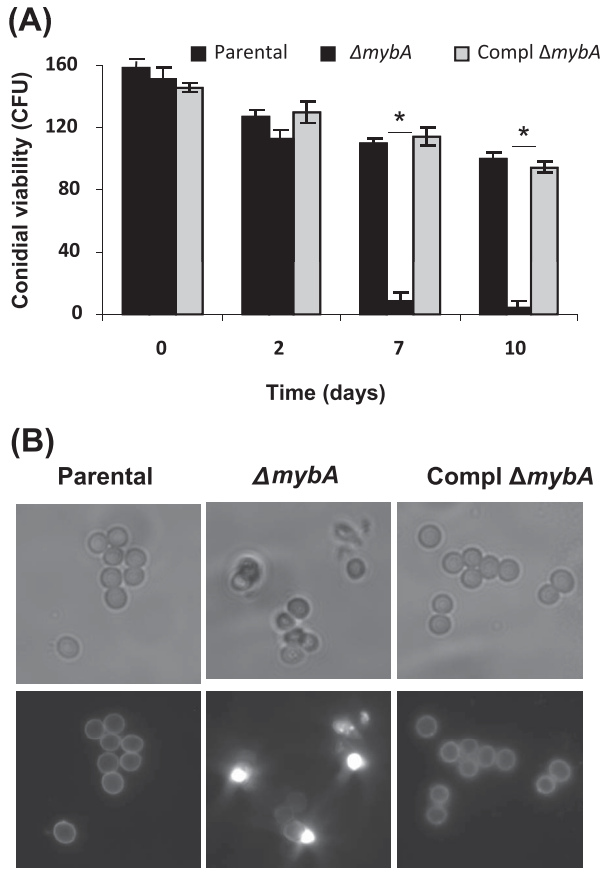

Fig. 4. Role of MybA in conidial viability.
A. Percentage of conidial viability upon storage at 20°C in water for 0, 2, 7 or 10 days. Estimation was done by plating the suspensions on solid 2% malt extract and counting CFU.
B. After 2 days of storage in water, conidia were labeled with 0.1 mg ml^{-1} FITC in 0.1M Na_2CO_3 pH9, for 30 min at 25°C. Note the bright intracellular fluorescence in the case of dead cells.

velC and *laeA*) while *brlA*, *stuA* and *medA* being even slightly up regulated (Supporting Information Table S1). In addition, it was verified by qRT-PCR that the expression of *mybA* was similar in the parental and in the Δ*abaA* and Δ*brlA* strains (Fig. 5C). The overexpression of *abaA* did not modify the expression of *mybA* (data not shown). These results indicated that *mybA* was not directly controlled by these two master regulators of the conidiation. Moreover, MybA did not control the expression of the *rodA* (AFUA_5G09580), which is at the most downstream position in the conidiation pathway (Supporting Information Table S1). Indeed, formic acid treatment normally used for the extraction of rodlets from the conidia could extract the same amount of the rodlet RodA protein was extracted from both the parental and Δ*mybA* strains (Supporting Information Fig. S9). To confirm that MybA was controlling the expression of *velB*, *vosA* or *wetA*, eight reporter strains were constructed with the promoter of *velB* or *vosA* or *wetA* or *tubA* (encoding tubulin used as a control) fused to the beta-D-glucuronidase reporter gene. Four parental and four Δ*mybA* mutant strains were transformed with the

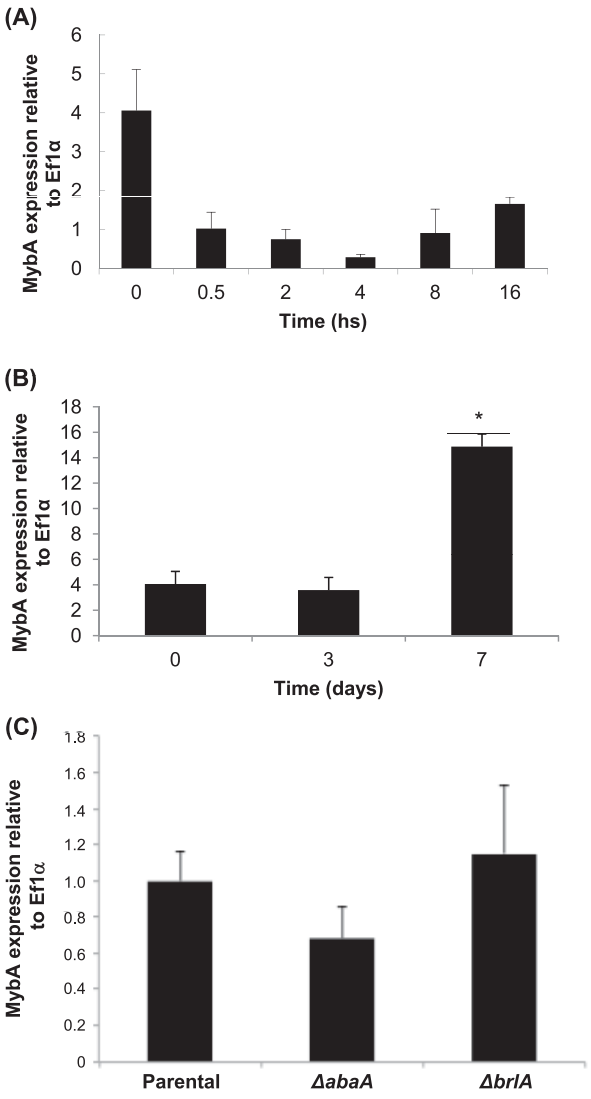

Fig. 5. Expression profile of MybA during vegetative and asexual development.
A. Expression levels during vegetative development were measured by qRT-PCR on RNA extracts from dormant conidia of the parental strain (0 h) and conidia that were incubated for 0.5, 2, 4, 8 or 16 h in liquid YPD at 37°C, 150 r.p.m. Gene expression data expressed as $2^{-\Delta\Delta Ct}$ are the mean of at least three replicates ± standard error and were calculated as the ratio of the target gene compared with the Elongation factor 1 (ef1α) gene used as a reference.
B. Expression levels during conidiophore development were estimated by qRT-PCR on RNA extracts from cultures at 25°C for 0, 3 or 7 days on cellophane membranes laid on solid 2% malt extract and inoculated with 10^6 conidia from the parental strain.
C. Expression of *MybA* in the two mutants of the central conidiation pathway (Δ*abaA*, Δ*brlA*). qRT- PCR data show that MybA is expressed in the Δ*abaA* and Δ*brlA* mutants at the same level as in the parental strain. Gene expression data expressed as $2^{-\Delta\Delta Ct}$ are the mean of at least 3 replicates ± standard error.

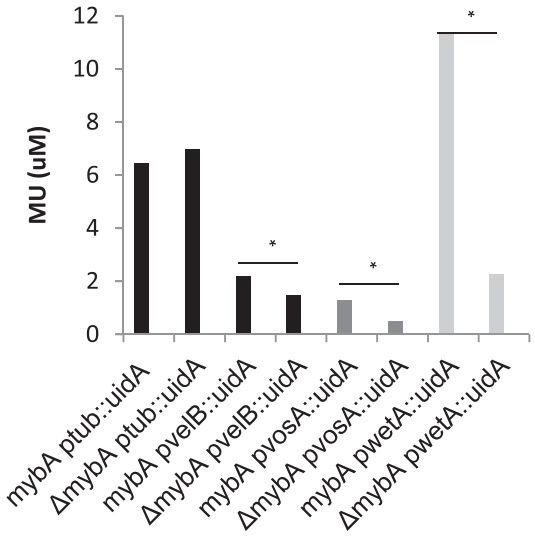

Fig. 6. MybA is controlling the expression of *wetA*, *vosA* and *velB* genes.
GUS assays were performed with parental and Δ*mybA* strains carrying the reporter gene β-glucuronidase (*uidA*) under the promoter of *velB* or *vosA* or *wetA* genes.

appropriate DNA construct inserted ectopically from the *mybA* locus at the biotin locus. The comparisons of the amount of 4-methylumbelliferone (MU) produced by the parental and Δ*mybA* strains carrying the same promoter-reporter construct showed that the expression of *wetA*, *vosA* and *velB* was strongly regulated by MybA while the expression of the control *tubA* was not affected by the *mybA* deletion (Fig. 6). The expressions of *wetA*, *vosA* and *velB* were respectively 5×, 2.5× and 1.5× higher in the parental strain than in Δ*mybA* strain. All together these data indicated that MybA is not controlled by the BrlA/AbaA central conidiation genes but is part of a second pathway situated downstream of the first pathway but controlling independently and differently conidiation and conidial maturation.

MybA is associated with cell wall metabolism

The RNA seq analysis showed that the only gene whose expression was totally switched off in the Δ*mybA* mutant was the *cspA* (AFUA_3G08990) which is a repeat-rich glycosylphosphatidylinositol-anchored cell wall protein previously analyzed by Levdansky *et al.* (2007). If the growth of both parental and Δ*cspA* mutant was normal, striking conidial phenotypes were also seen in the Δ*cspA* mutant constructed in the Ku80/CEA17 background (while these phenotypes have not been described before in the Δ*cspA* mutant constructed in the Afu293 background and analyzed by Levdansky *et al.* (2007). The Δ*cspA* mutant conidia tended to stay grouped together in long chains when they were recovered from the agar slant in a 0.05% Tween-20 aqueous solution while the conidia of the parental strain were separated. Linear conidial chains also adhered between themselves in the mutant (Supporting Information Fig. S10). The conidia of the Δ*cspA* mutant germinated faster than their parental strain (Fig S11). Moreover, the conidial viability of the Δ*cspA* mutant was affected (Supporting Information Fig. S11); an increased intracellular CFW staining of the mutant conidia indicated the death of the intracellularly stained conidia (Supporting Information Fig. S10). The faster germination and increased permeability of the Δ*cspA* mutant were similar to the phenotype of the Δ*mybA* mutant.

The defects in survival and cell wall permeability associated with the Δ*cspA* and Δ*mybA* mutants suggested that the deletion of the *mybA* gene affected the organization of the conidium cell wall. The deletion of *mybA* was indeed associated with the upregulation of many cell wall biosynthesis genes (116/358 *in silico* identified) (Supporting Information Table S1). The Δ*mybA* RNA-seq showed that all α- and β-1,3-glucan synthase, and several chitin synthase genes were upregulated (Table 1). In addition, the expression of many cell wall remodelling enzymes as well as cell wall polysaccharide degrading enzymes (α-/β-1,3-glucanases and chitinases) was also affected in the Δ*mybA* mutant. The polysaccharide composition of the conidial cell wall was indeed modified in the Δ*mybA* mutant (Supporting Information Fig. S12). Chitin and α-glucan were significantly higher in the mutant than in the parental strain. The amount of the β-1,3-glucan was reduced in the Δ*mybA* mutant even though the expression of fks1 was higher in the mutant. This could be associated with high increase in the expression of β-1,3-glucanases such as the SUN protein (Gastebois *et al.*, 2013) and the putative exoglucanases of the GH3 family AFUA_6G08700 and AFUA_7G06140 with GFOLD values >2. These data also confirmed the lack of role of the endo β-1,3-glucanases of the families GH81 and GH16 in the remodelling of the mycelial cell wall (Mouyna *et al.*, 2016). The GFOLD analysis indicated that the expression of the genes involved in the melanin biosynthesis pathway was not significantly affected by the deletion of *mybA*. This was in agreement with the biochemical and TEM data showing that the amount of the pigment solubilized by H_2O_2 at 65°C of the parental and Δ*mybA* mutant was similar in both strains (Supporting Information Fig. S13). Although the Δ*mybA* mutant conidia were hydrophilic, the amount of the rodlet RodA protein extractable from the Δ*mybA* mutant conidia was similar to that of the parental strain (Supporting Information Fig. S9). Incubation of the conidia of the Δ*mybA* mutant with 0.5 M NaCl for a short

Table 1. Gene expression of cell wall biosynthesis genes in the Δ*mybA* mutant and parental strain (WT) (values are taken from the RNA-seq data analysis).

Accession number	Annotation	GFOLD Value (Δ*mybA*/WT)	WT RPKM	Δ*mybA* RPKM
AFUA_6G12400	1,3-beta-glucan synthase catalytic subunit FksP	1.33	45.65	161.64
AFUA_6G06900	Rho GTPase Rho1	1.05	364.03	1076.90
AFUA_2G01170	1,3-beta-glucanosyltransferase Gel1	0.97	150.90	424.69
AFUA_6G11390	1,3-beta-glucanosyltransferase Gel2	0.84	14.83	53.07
AFUA_2G12850	1,3-beta-glucanosyltransferase Gel3	0.33	14.13	35.08
AFUA_2G05340	1,3-beta-glucanosyltransferase Gel4	1.20	86.52	294.82
AFUA_3G13200	1,3-beta-glucanosyltransferase Gel6	−0.15	40.38	31.55
AFUA_6G12410	1,3-beta-glucanosyltransferase Gel7	0	0	0.46
AFUA_8G02130	1,3-beta-glucanosyltransferase Gel5	0	5.37	14.10
AFUA_1G13940	SUN domain protein Sun2	0	1.36	3.33
AFUA_7G05450	SUN beta-1,3-glucanase Sun1	3.21	5.41	166.46
AFUA_6G12380	cell wall glucanase Scw4	−1.23	23.42	8.98
AFUA_1G11460	1,3-beta-glucanosyltransferase Bgt1	1.75	54.54	308.31
AFUA_3G00270	cell wall glucanase, putative Bgt2	1.61	35.18	182.87
AFUA_8G05610	cell wall glucanase Scw11	2.84	8.32	127.91
AFUA_5G08780	cell wall glucanase, putative Bgt3	0.56	14.44	39.67
AFUA_1G04260	GH81 endo-1,3-beta-glucanase Engl1	−0.58	29.29	18.00
AFUA_2G14360	GH16 endo-1,3-beta-glucanase, Eng2	−1.10	43.74	18.43
AFUA_1G05290	GH16 endo-1,3(4)-beta-glucanase, Eng3	−0.72	47.64	24.23
AFUA_5G02280	GH16 endo-1,3-beta-glucanase eng4	−0.20	19.65	16.15
AFUA_4G13360	GH16 endo-1,3-beta-glucanase, Eng5	−1.83	3.39	1.16
AFUA_6G14540	GH16 endo-1,3-beta-glucanase eng6	0	0	0.22
AFUA_3G03080	GH16 endo-1,3-beta-glucanase Eng7	−1.64	11.22	4.38
AFUA_5G14030	GH16 endo-1,3-beta-glucanase, Eng8	−1.42	2.11	0.96
AFUA_6G08700	putative exo beta-1,3-glucanase	2.73	9.02	114.87
AFUA_7G06140	putative exo beta-1,3-glucanase	2.20	4.34	55.40
AFUA_1G14450	exo-beta-1,3-glucanase Exg0	−0.24	36.90	29.69
AFUA_2G00430	exo-beta-1,3-glucanase, putative	0	0.32	1.31
AFUA_3G07520	exo-beta-1,3-glucanase, putative	0.87	5.55	22.99
AFUA_4G03350	exo-beta-1,3-glucanase, putative	0.96	8.64	34.00
AFUA_6G11980	exo-beta-1,3-glucanase, putative	−2.16	2.34	0.08
AFUA_6G13270	exo-beta-1,3-glucanase, putative	−1.04	26.31	10.98
AFUA_1G16190	cell wall transglycosidase Crf1	0.75	64.02	171.60
AFUA_3G09250	cell wall transglycosidase Crh1–2	−0.20	64.36	50.29
AFUA_6G03230	cell wall transglycosidase Crh1–3	−0.74	17.93	11.21
AFUA_6G08510	cell wall transglycosidase Crh1–4	1.12	15.65	67.83
AFUA_2G03120	cell wall transglycosidase Crh2	0.15	88.18	148.95
AFUA_1G01730	Cell wall putative transglycosidase Dfg1	0.12	23.12	46.54
AFUA_2G00680	Cell wall putative transglycosidase Dfg2	−0.48	26.46	16.01
AFUA_3G00340	Cell wall putative transglycosidase Dfg3	0.09	7.02	21.40
AFUA_3G00700	Cell wall putative transglycosidase Dfg4	0	4.83	10.11
AFUA_3G02040	Cell wall putative transglycosidase Dfg6	0.25	0.63	6.26
AFUA_4G00620	Cell wall putative transglycosidase Dfg5	−0.47	22.62	13.67
AFUA_4G02720	Cell wall putative transglycosidase Dfg7	0	7.94	22.19
AFUA_4G06820	related to sporulation-specific gene SPS2, Ecm33	0.68	415.03	901.18
AFUA_1G15440	alpha-1,3-glucan synthase Ags3	0.93	37.37	100.17
AFUA_2G11270	alpha-1,3-glucan synthase Ags2	1.90	2.25	17.82
AFUA_3G00910	alpha-1,3-glucan synthase Ags1	1.17	18.82	62.97
AFUA_1G00650	alpha-1,3-glucanase, putative	0	0	0
AFUA_2G03980	alpha-1,3-glucanase, putative	0	1.94	5.05
AFUA_5G03940	alpha-1,3-glucanase, putative	−1.04	50.26	21.18
AFUA_7G08350	alpha-1,3-glucanase, putative	0	0	0
AFUA_7G08510	alpha-1,3-glucanase, putative	0	0	1.00
AFUA_8G06030	alpha-1,3-glucanase, putative	−1.02	26.35	10.29
AFUA_2G06160	alpha(1,3)glucanase	0	1.93	2.27
AFUA_8G06360	alpha-1,3-glucanase, putative	0	0	0.25
AFUA_5G02740	alpha-1,2-mannosyltransferase Ktr1	−0.11	68.54	58.43
AFUA_5G10760	alpha-1,2-mannosyltransferase Kre2	−0.30	40.82	27.83
AFUA_5G12160	alpha-1,2-mannosyltransferase Ktr5	0.24	81.02	144.91
AFUA_2G11870	mannosyltransferase Kre6	−0.66	19.91	10.05
AFUA_6G04450	alpha-1,2-mannosyltransferase Mnn2	−2.62	59.12	7.99
AFUA_5G13090	alpha-1,2-mannosyltransferase, putative Mnn2	0	2.60	6.61
AFUA_6G14480	mannosyltransferase, putative Mnn1	0.82	6.56	32.56
AFUA_2G01450	alpha-1,6 mannosyltransferase subunit Mnn9	−1.35	126.60	48.04

Table 1: *Continued*

Accession number	Annotation	GFOLD Value (Δ*mybA*/WT)	WT RPKM	Δ*mybA* RPKM
AFUA_1G01380	alpha-1,6-mannosyltransferase subunit Och1–4	0.35	29.46	71.52
AFUA_2G14910	alpha-1,6-mannosyltransferase subunit Mnn10	0.05	14.56	30.73
AFUA_4G10750	alpha-1,6-mannosyltransferase subunit Mnn11	−0.12	73.44	60.72
AFUA_5G08580	alpha-1,6-mannosyltransferase subunit Och1–1	−2.03	133.34	31.49
AFUA_6G14040	alpha-1,6-mannosyltransferase subunit Och1–2	0	0	5.38
AFUA_8G02040	alpha-1,6-mannosyltransferase subunit Och1–3	1.66	11.37	81.25
AFUA_2G15910	mannosyltransferase, putative van1	−1.66	200.31	64.93
AFUA_1G12630	mannosylphosphate transferase Mnn4	−0.67	20.26	13.75
AFUA_1G03790	mannosylphosphorylation protein Mnn4	−1.60	61.37	16.70
AFUA_1G12040	chitin biosynthesis protein Chs7	0.81	18.37	66.84
AFUA_6G02510	chitin biosynthesis protein Chs5	0	13.31	18.75
AFUA_3G05580	chitin synthase activator Chs4	0.27	30.02	59.24
AFUA_6G02940	chitin synthase activator Chs4	0.09	34.92	58.02
AFUA_8G05620	chitin synthase activator Chs4	1.03	8.45	35.77
AFUA_2G01870	chitin synthase A	0	45.36	52.48
AFUA_4G04180	chitin synthase B	0.15	9.17	19.01
AFUA_5G00760	chitin synthase C	0	18.72	25.82
AFUA_1G12600	chitin synthase D	0	0.44	3.28
AFUA_2G13440	chitin synthase E	0.28	29.51	52.75
AFUA_8G05630	chitin synthase F	0.72	10.31	30.26
AFUA_3G14420	chitin synthase G	0.76	35.19	91.90
AFUA_2G13430	chitin synthase, EB	0.87	21.19	58.87
AFUA_5G03760	class III chitinase ChiA1	4.52	10.83	459.40
AFUA_8G00700	class III chitinase ChiA2	0	17.24	23.20
AFUA_3G07110	class III chitinase, putative ChiA5	−0.15	7.77	8.54
AFUA_5G03530	class III chitinase, putative ChiA4	−1.81	22.55	4.07
AFUA_5G03850	class III chitinase, putative Cts1	0	43.12	41.33
AFUA_7G05140	class III chitinase, putative ChiA3	−0.13	17.15	14.80
AFUA_5G03960	class V chitinase Chi100	1.96	21.85	131.31
AFUA_8G01410	class V chitinase ChiB1	0	11.09	20.22
AFUA_1G00310	class V chitinase, putative Cts2	0	0	0
AFUA_1G02800	class V chitinase, putative Cts2	0.19	19.84	44.99
AFUA_3G07160	class V chitinase, putative Cts2	−1.02	92.44	43.16
AFUA_3G11280	class V chitinase, putative Cts2	1.89	24.19	162.49
AFUA_5G01400	class V chitinase, putative Cts2	0.13	0	2.61
AFUA_5G06840	class V chitinase, putative Cts2	0	2.22	2.88
AFUA_6G09310	class V chitinase, putative Cts2	1.43	4.70	35.52
AFUA_6G09780	class V chitinase, putative Cts2	0	0	0
AFUA_6G13720	class V chitinase, putative Cts2	0	0.23	0.59
AFUA_7G08490	class V chitinase, putative Cts2	0	0	0
AFUA_3G12690	UDP-Galactose épimerase Ugm1	0.91	5.90	31.23
AFUA_6G02120	beta-1,5 galactofuranosyltransferase	0.94	10.74	43.23
AFUA_3G07860	glycosyl transferase, putative GT4C	0.60	7.45	18.32
AFUA_3G07890	Ega3, alpha-1,4 galactosaminidase	0.60	81.49	196.31
AFUA_3G07900	Sph3, Spherulin-like protein	1.32	11.81	76.73
AFUA_3G07870	Agd3, putative deacetylase	1.81	30.81	171.33
AFUA_4G14070	glycosyl transferase, putative GT4B	1.84	24.62	125.75
AFUA_3G07910	UDP-glucose 4-epimerase, putative Uge3	1.19	1.50	19.43
AFUA_5G10780	UDP-glucose 4-epimerase Uge5	0	94.90	117.12

GFOLD values less than −1 and greater than 1 are considered significantly downregulated and upregulated in the Δ*MybA* mutant respectively.

time resulted in the release of proteins while no protein could be extracted from the conidia of the parental strain (Supporting Information Fig. S14). This result indicated that the conidia of the Δ*mybA* mutant, similar to the conidia of the Δ*ags* and Δ*alb1* mutants (Beauvais *et al.*, 2013; Bayry *et al.*, 2014) were covered by a layer of (glyco)proteins which make these conidia hydrophilic. All the modifications noticed in the composition and structure of the Δ*mybA* mutant conidial cell wall could be responsible for the increased cell wall permeability seen in the conidia of the Δ*mybA* mutant. These data confirmed that MybA plays an important role in controlling the conidial cell wall integrity.

MybA is involved in the regulation of trehalose metabolism

The conidial phenotype of the Δ*mybA* strain was reminiscent of several mutants that all showed a reduction (or even complete loss) of the conidial trehalose content

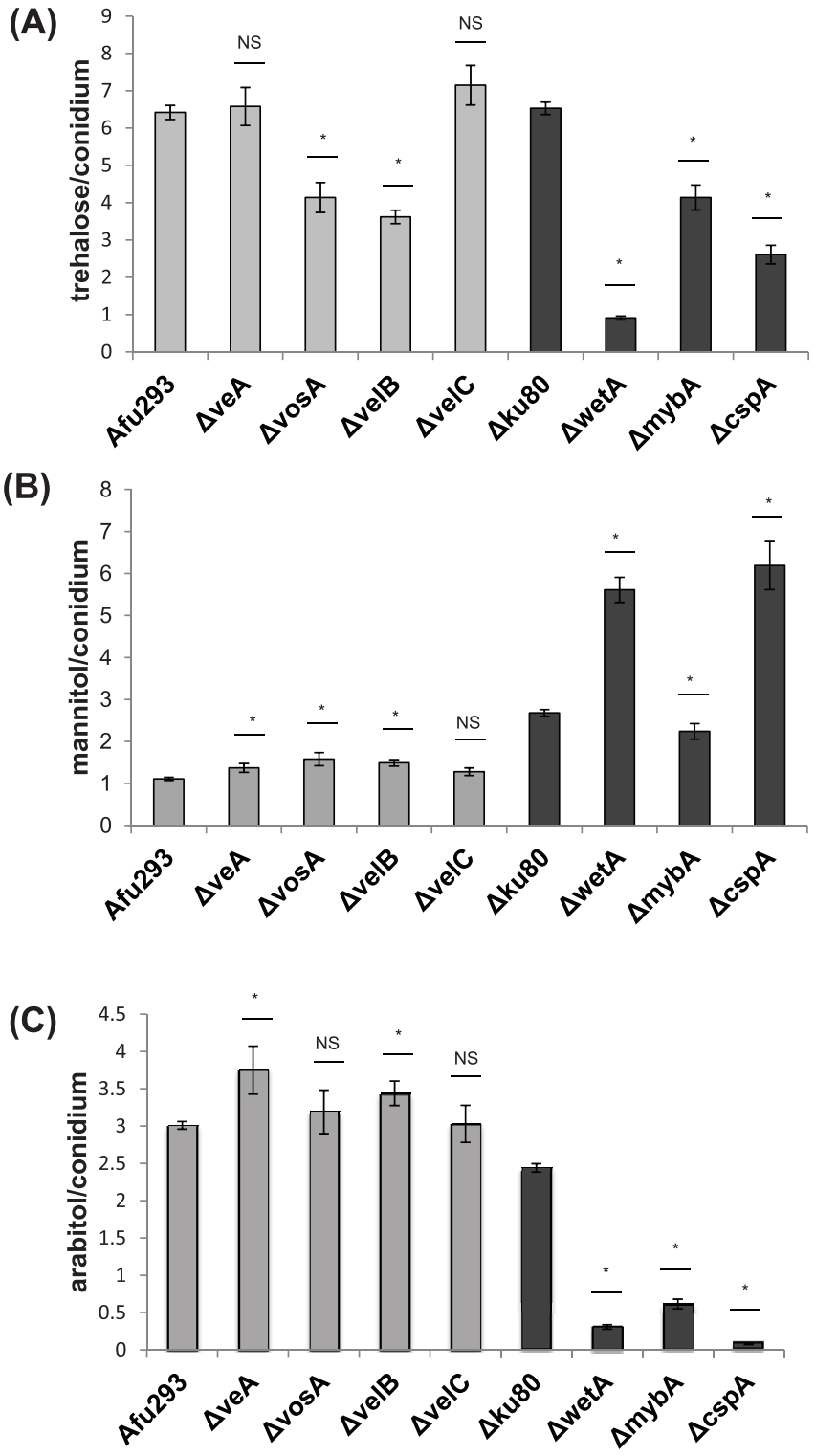

Fig. 7. Trehalose and polyols content of conidia from Δ*veA*, Δ*vosA*, Δ*velB*, Δ*velC* mutants with their parental strain (*Afu293*), and Δ*wetA*, Δ*mybA* and Δ*cspA* mutants and their Δ*ku80* parental strain. The amount of trehalose and polyols in freshly collected 9-day-old conidia was determined by HPLC following conidial breakage. Concentration of trehalose (A), mannitol (B) arabitol (C) were calculated. Concentrations are given in mg $\times 10^{-7}$/ conidium. Starts (*) means significantly different with respect to parental strain. The *p* values with respect to parental strains for (A) are: Δ*veA* $p = 0.6326$ NS, Δ*vosA* $p = 0.0009$ S, Δ*velB* $p = <0.0001$ S, Δ*velC* $p = 0.0879$ NS, Δ*wetA* $p < 0.0001$ S, Δ*mybA* $p = 0.0001$ S, Δ*cspA* $p < 0.0001$ S; for (B) Δ*veA* $p = 0.0467$ S, Δ*vosA* $p = 0.0145$ S, Δ*velB* $p = 0.0077$ S, Δ*velC* $p = 0.1325$ NS, Δ*wetA* $p < 0.0001$ S, Δ*mybA* $p = 0.0126$ S, Δ*cspA* $p = 0.0005$ S and (C) Δ*veA* $p = 0.0237$ S, Δ*vosA* $p = 0.4962$ NS, Δ*velB* $p = 0.0269$ S, Δ*velC* $p = 0.8662$ NS, Δ*wetA* $p < 0.0001$ S, Δ*mybA* $p < 0.0001$ S, Δ*cspA* $p < 0.0001$ S.

associated with a decrease in conidial viability (Tao and Yu, 2011; Park *et al.*, 2012a, 2012b). In addition, the RNA-seq data indicated that the trehalose biosynthetic process (GO 0005992) was significantly overrepresented in the genes with a GFOLD lower than −1.5 (Table 2). The trehalose content of 9-day-old conidia was therefore quantified in the Δ*mybA* mutant and compared with that of the Δ*velC*, Δ*velB*, Δ*veA*, Δ*vosA*, Δ*wetA and* Δ*cspA* mutants (Fig. 7A; Supporting Information Fig. S15). The Δ*wetA* and Δ*cspA* mutants had

Table 2. Gene expression of genes involved in trehalose metabolism in the Δ*mybA* mutant and parental strain (values are taken from the RNA-seq data analysis).

Accession numbers	Annotation	GFOLD (Δ*MybA*/WT)	WT RPKM	Δ*mybA* RPKM
AFUA_6g12950	alpha,alpha-trehalose-phosphate synthase subunit TpsA	−0.80	275.52	170.20
AFUA_2g04010	alpha,alpha-trehalose-phosphate synthase tpsB	−1.60	223.31	76.27
AFUA_4g03190	alpha,alpha-trehalose-phosphate synthase TpsC	0	0	0
AFUA_3g02280	alpha,alpha-trehalose glucohydrolase, putative TreA	0.60	14.66	37.97
AFUA_4g13530	Trehalase TreB	−1.21	186.93	86.60
AFUA_2g04020	alpha,alpha-trehalose phosphate synthase	−0.58	107.21	75.31
AFUA_5g14300	alpha,alpha-trehalose-phosphate synthase	−1.88	23.55	5.13
AFUA_3g05650	alpha,alpha-trehalose-phosphate synthase subunit	−1.35	154.38	64.60
AFUA_7g03940	alpha,alpha-trehalose phosphate synthase subunit	−2.07	501.58	134.21
AFUA_3g12100	trehalose phosphorylase	−1.70	212.41	69.36
AFUA_5g14780	trehalose phosphorylase	−3.33	36.03	2.63

GFOLD values less than −1 and greater than 1 are considered significantly downregulated and upregulated in the Δ*mybA* mutant respectively.

the lowest amount of trehalose, 13% and 40% of the parental strain respectively. To a lesser but to a significant extent Δ*mybA*, Δ*velB* and Δ*vosA* had a significant reduction of the trehalose content (about 50%) compared with the parental strain. These data were in agreement with a tight regulation of these trehalose genes by the *mybA* gene. In contrast, the deletion of *velC* and *veA* genes which are not controlled by *mybA*, was not associated with a reduction in conidial trehalose in the respective mutant strains. The two methods used to quantify the amount of trehalose gave the same trehalose amount (Fig. 7, Supporting Information Fig. S15). This result was in agreement with the RNA-seq data that showed that the *cspA, wetA*, *velB* and *vosA* genes were controlled (at least partially) by MybA protein. Moreover, it indicated that MybA was involved in the regulation of the trehalose metabolism. In *A. fumigatus*, two different pathways have been proposed to be involved in the trehalose biosynthesis (Lamarre *et al*., 2008; Al-Bader *et al*., 2010; Puttikamonkul *et al*., 2010). In the first pathway, glucose-6-phosphate and UDP-glucose are transformed by trehalose-6-phosphate synthases into trehalose-6-phosphate and a phosphate group is removed from the trehalose-6-phosphate by a trehalose-6-phosphate phosphatase to yield trehalose. *In silico* GFOLD analysis has shown that most genes assigned to the trehalose-6-P-synthases and phosphatase complex (AFUA_6G12950, AFUA_2G04010, AFUA_2G04020, AFUA_4G03190 and AFUA_5G14300, AFUA_3G05650, AFUA_7G03940) were significantly down regulated (Table 2). This down regulation of the genes involved in the trehalose pathway which has been noticed in the RNA-seq data (Table 2) was confirmed by qRT-PCR experiments (data not shown). In the second pathway involved in the synthesis of trehalose in *A. fumigatus*, trehalose phosphorylases produce trehalose from glucose-6-phosphate and glucose. The expression levels of the two trehalose phosphorylases associated with this pathway (AFUA_3G12100 and AFUA_5G14780) were also reduced in the Δ*mybA* mutant; the AFUA_5G14780 gene being one of the most down regulated genes (GFOLD = −3.33). The down regulation of the genes involved in the synthesis of the trehalose was in agreement with the lower amount of trehalose found in the conidium of the Δ*mybA* mutant strain.

The other conidial polyols varied differently from the trehalose in the Δ*mybA*, Δ*velC*, Δ*velB*, Δ*veA*, Δ*vosA*, Δ*wetA* and Δ*cspA* mutants (Fig. 7B). The Δ*wetA* and Δ*cspA* mutants had a very high amount of mannitol (>3× the concentration of the parental strain) whereas the Δ*vosA*, Δ*velB* and Δ*mybA* mutants showed only a slight difference in the mannitol level with respect to the parental strain. Δ*cspA*, Δ*wetA* and Δ*mybA* mutants had a very low amount of arabitol whereas the Δ*vosA* and Δ*velB* had an amount similar to the parental strain (Fig. 7C). These results suggest that the conidial intracellular osmolytes are controlled by compensatory pathways, which are differently activated in the different conidiating mutant strains.

MybA is involved in scavenging *intracellular ROS*

ROS scavenging enzymes can play a major role in protecting the fungus against apoptotic death induced by stress. In agreement, there was a down regulation of ROS scavenging enzymes such as the conidial catalases (*catA* AFUA_6G03890; GFOLD = −3.92 and AFUA_2G00200; GFOLD = −4.94) and the superoxide dismutase AFUA_1G11640 (GFOLD = −1.99) were down regulated in the Δ*mybA* mutant (Supporting Information Table S1). The use of the Mitochondrial Superoxide Indicator dye MitoSOX confirmed that indeed the Δ*mybA* strain had 27% more mitochondrial superoxide

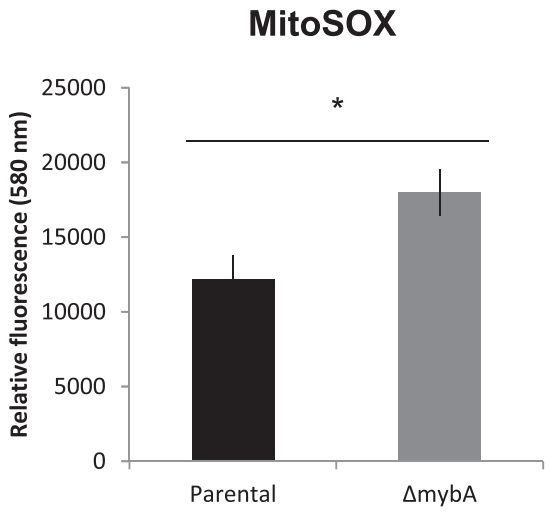

Fig. 8. ROS scavenging enzymes are down regulated in the Δ*mybA* mutant.
Equal amount of conidia were grown in RPMI (without phenol red) for 19 h at 37°C, and then MitoSOX was added for 15 min. The Relative Fluorescence Units was calculated by taken the fluorescence units a 580 nm subtracting the fluorescence of cells in RPMI without MitoOX.

anion than the parental strain (Fig. 8). The dehydrin *dprA* (AFUA_4G00860) which controls the response to oxidative stress in the conidia (Wong Sak Hoi *et al.*, 2011) was significantly down regulated in the Δ*mybA* strain (GFOLD= −0.17). These results suggested that the survival of the conidia depends on the activity of scavenging enzymes controlling the intracellular release of ROS during an active metabolic process such as conidiation. The impact of MybA on controlling the intracellular oxido-reduction potential was confirmed by the high expression of genes from the GO0055114, GO0016491, GO0016705, GO0004497 all characterized by oxidoreductase or monooxygenase activity.

The ΔmybA *mutant strain is defective in virulence*

It was hypothesized that the inability of Δ*mybA* mutant to sustain an increased intracellular ROS induced by a stress, and the altered cell wall permeability of the Δ*mybA* conidia could be associated with a defect in survival and subsequent virulence of the Δ*mybA* mutant in mice. Indeed, the Δ*mybA* conidia were more susceptible to the killing by phagocytes at 36 h after intranasal inoculation to immunocompetent mice (Fig. 9A). Moreover, in an experimental murine model of invasive aspergillosis with cyclophosphamide treatment, the Δ*mybA* mutant strain was less virulent than the parental and the complemented Δ*mybA* strains (Fig. 9B). Starting from day 4-post infection, a significant difference between the parental *versus* the Δ*mybA* strain was observed for the weight loss (data not shown) as well as for the survival. With an inoculum of 5×10^4 conidia, all mice died after 5 days ($p < 0.005$) when infected with parental or complemented Δ*mybA* strains, but not those mice i.n. inoculated with the Δ*mybA* mutant conidia. These results proposed that MybA plays important role in controlling the virulence of *A. fumigatus*.

Discussion

Positioning of MybA in the conidiogenesis regulation pathway

Myb transcription factors account for a small proportion of the overall transcription factors annotated in the *A. fumigatus* genome: in this species, 25 Myb TFs were annotated among the 576 putative transcription factors identified in the FTFD database. To our knowledge, only one transcription factor belonging to the Myb family FlbD, was studied so far in *Aspergillus*, where it regulates asexual and sexual development (Wieser and Adams, 1995; Arratia-Quijada *et al.*, 2012). The nuclear

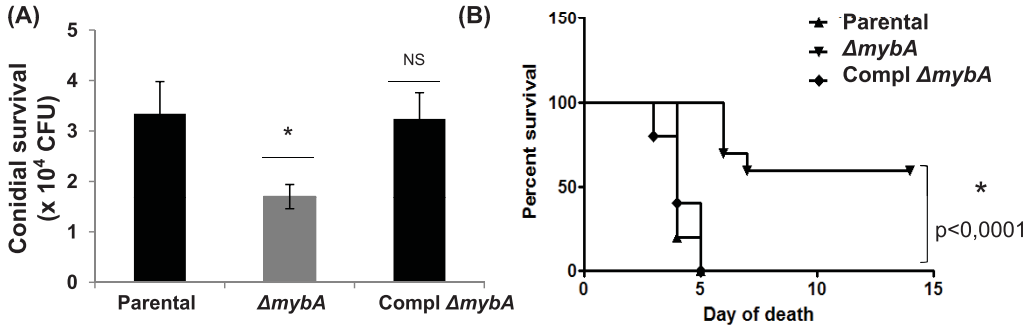

Fig. 9. Survival and growth of *A. fumigatus* conidia in immunocompetent and immunocompromised mice.
A. Conidial survival was evaluated by plating serial dilutions of bronchoalveolar lavages 36 h after intranasal inoculation of immunocompetent mice with 5×10^8 per mouse. Data are the mean value obtained with 3 mice ± standard error.
B. Survival of mice infected with conidia of Δ*mybA* or parental strain or complemented Δ*mybA*. Cohorts of 10 mice immunosuppressed by cyclophosphamide were inoculated with 5×10^4 conidia per mouse. Mice were considered dead when their weight was equal to 10 g.

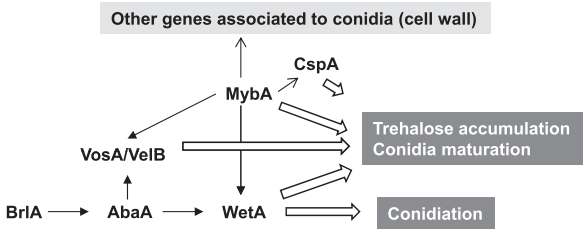

Fig. 10. Proposed model for the position of MybA in the conidiation pathway in *A. fumigatus*.

localization of MybA was confirmed here by its association with importins after two different pull-down experiments. Importins bind to nuclear localization signals in their protein cargos to transport them through nuclear pore complexes into the nucleus. In yeast, importin α (Kap60) binds to the NLS and importin β (Kap95) stabilizes the interaction and in turn binds to FG-repeat-containing nucleoporins. Ran-GTP provides an important source of energy to the reaction by binding to importin (Aitchison and Rout, 2012; Soniat and Chook, 2015). The same role can be expected for the importin α and β of *A. fumigatus* and the GTPase recovered by immunoprecipitation even though it is different from the *A. fumigatus* Ran GTPase, may provide some energy for the entrance of the complex to the nucleus. Based on the described pathways involved in the regulation of the temporal and spatial expression of conidiophore development and conidial maturation-specific genes on the one hand, and on our functional analysis of MybA on the other hand, we propose an updated model for the regulation of conidiation in *A. fumigatus* (Fig. 10) which is based on two major findings of the Δ*mybA* transcriptome analysis: (1) the expression of *mybA* was not down regulated in the Δ*brlA* and Δ*abaA* mutants and (2) the expression of *wetA*, *velB* and *vosA* were downregulated in the Δ*mybA* mutant, indicating that WetA, VelB and VosA acted downstream of MybA. The analysis of the sequences of the promoters of *wetA*, *vosA* and *velB* using the promoter eukaryotic GPMiner programme software (www.molbiol-tools.ca), putatively identified two palindromic sequences (CAGTT and AACTG) in the promoters of these three genes which could be a binding site for MybA (data not shown). However, the regulation of these three genes by *mybA* was light independent. A clear picture of the control of conidiation in *Aspergillus* is still incomplete.

mybA *mutation results in the production of conidia affected in dormancy*

A major reason for the loss of viability of the Δ*mybA* conidia was due to the reduction in the amount of trehalose in the conidium. Trehalose is a non-reducing disaccharide that is synthesized by a wide variety of organisms (bacteria, plants, insects and fungi). Trehalose constitutes up to 15% of the dry weight of vegetative resting cells and spores (Elbein, 1974), where it functions both as a reserve carbohydrate and a stress metabolite (Thevelein and Hohmann, 1995; Arguelles, 2000). It was known that several *Aspergillus* conidiation mutants with a reduced trehalose content showed impaired viability of their conidia, as illustrated by the mutants of the trehalose-6-phosphate synthase (*tpsA* (Fillinger *et al*., 2001)), of the regulator VosA, VelB (Ni and Yu, 2007; Park *et al*., 2012a, 2012b), and of the transcription factor WetA (Tao and Yu, 2011). Together with the results on Δ*mybA* mutant, these data indicated that the lack of trehalose in the fungal conidia of Δ*mybA* results in the rapid loss of viability. The increase in the mannitol concentration, moderate in the Δ*mybA* or very high in the Δ*wetA* was not sufficient to compensate for the loss of trehalose in these conidiation mutants. Accordingly, Wyatt *et al*. (2014a, 2014b, 2014c) have recently shown that deletion in the mannitol phosphate dehydrogenase that resulted in the absence of mannitol in the conidia, was not affecting conidia in *Neosartorya fischeri*, a species very close to *A. fumigatus*.

Another pathway putatively involved in the conidial dormancy is the tight regulation of water influx/efflux in the spores. Hydrophilins have been associated with the survival of plants and fungi during water deficient periods (Wong Sak Hoi *et al*., 2011). During conidial maturation, the fungus has to cope with the dehydration process to reach a metabolism that is minimal in the dormant conidium (Lamarre *et al*., 2008). Hydrophilins that participate in this process have a high glycine content with anhydrophilicity index >1 and are completely unfolded (Garay-Arroyo *et al*., 2000; Welker *et al*., 2010; Lopez-Martinez *et al*., 2012; Suzuki *et al*., 2013). Hsp9 (=Awh11) (AFUA_1G17370) and Con10 (AFUA_6G03210) which are two members of this hydrophilin family, were especially downregulated in the Δ*mybA* mutant, with GFOLD values of -4.4 and -3.1 respectively. We hypothesized that the down regulation of the hydrophilins could be correlated to a reduced survival of the conidium during anhydrobiosis. The deletion of the *awh11* gene was successfully undertaken while we were unable to construct a Δ*con10* mutant (data not shown). The Δ*awh11* mutant strain germinated and grew like the parental strain. The only phenotype seen with the Δ*awh11* strain was an increase in the resistance to freezing (data not shown). Similarly, the hydrophilin *dprC* (AFUA_7G04520), which is involved in the resistance to freezing, was also down regulated in the Δ*mybA* mutant strain (GFOLD $=-1.7$) (Wong Sak Hoi *et al*., 2012). Other proteins involved in water influx such as the aquaglyceroporins AFUA_4G00680 and AFUA_4G03390 (Supporting Information Table S1) were also down regulated. However, the deletion of the genes

encoding these aquaglyceroporins did not result in the production of conidia affected in their survival (data not shown). To date, it was not possible to demonstrate a direct role of MybA in controlling water influx/efflux during conidial storage.

Another reason for the loss of conidial viability in the Δ*mybA* mutant could be a defect in the cell wall permeability resulting from an alteration in the structural organization of the cell wall. The impact of conidiation regulators on cell wall biosynthesis has been documented in other occasions. Tao and Yu (2011) have shown that the Δ*wetA* mutant conidia have an altered cell wall but the cell wall changes have not been biochemically characterized. Recent studies have shown that the velvet proteins of *Histoplasma capsulatum* associated with DNA drive the expression of temperature responsive genes controlling dimorphism associated with cell wall changes in this species (Beyhan *et al.*, 2013). Many genes important for cell wall integrity are affected by the *mybA* deletion. For example, the deletion of the *cspA* gene that is controlled by MybA resulted in the weakening of the conidial cell wall (Levdansky *et al.*, 2010). The expression of the genes associated with polysaccharide synthesis, remodelling and hydrolysis were differentially regulated in the Δ*mybA* mutant suggesting a direct effect of MybA on cell wall polysaccharide synthesis which could be responsible for the cell wall permeability defect in the Δ*mybA* mutant (Table 1). However, our biochemical and structural data showed that the melanin and RodA outer-layer of the conidium cell wall was not affected and that the permeability defect in the Δ*mybA* mutant was mainly associated with the modification of the inner fibrillar cell wall layer. In contrast, the Δ*wetA* mutant which has also conidia with altered survival, has a cell wall conidia with a reduced amount of melanin and altered rodlet layer (Tao and Yu, 2011). These results suggested that MybA and WetA control the conidial cell wall biosynthesis differently. WetA would regulate mainly the construction of the outer layer since the melanin and rodlets are affected in this mutant. In contrast, MybA would control mainly the synthesis of the inner layer without modifying the outer layer. These results also suggested that the cell wall glucan and chitin and trehalose synthesis could be linked. Both pathways have a common precursor which is glucose-6-phosphate and an increase in the glucose phosphate pool due to the lack of consumption for trehalose synthesis may lead to the production of nucleotide sugars to be used by the cell wall biosynthetic genes.

Impact of the mybA *deletion on global metabolic pathways*

Although it was shown that the Δ*mybA* mutant conidiation was affected by heat, only five genes coding for putative heat shock proteins were down regulated in the Δ*mybA* mutant among the 22 genes annotated as heat shock protein or identified by proteome analysis (Albrecht *et al.*, 2010). These genes were *awh11* (AFUA_1G17370), *hsp30* (AFUA_3G14540), *hsp78* (AFUA_1G11180), *hsp20* (AFUA_5G10270) and *hsp12* (AFUA_6G12450) with GFOLD values of −4.4, −2.0, −1.6, −1.4, −1.4 respectively. Interestingly, most of the downregulated Hsps were small Hsp proteins. Moreover, one of them encoded by AFUA_1G11180 was shown to play the most active role in transcription regulation at 48°C (Do *et al.*, 2009). The expression of all the other Hsp proteins was not modified in the Δ*mybA* mutant or even upregulated for six of them.

The RNA seq analysis suggested that MybA has an impact on the global physiology of *A. fumigatus*. For example, the nitrate reductase metabolism was down regulated in the Δ*mybA* mutant. The nitrate reductases (AFUA_3G15190, AFUA_5G10420 and AFUA_1G12830) and the nitrite reductase AFUA_1G12840 were all down regulated with respective GFOLD values of −1.5, −3.9, −2.0 and −1.1. Other studies (Lopez-Berges *et al.*, 2014) have also shown that velvet proteins (controlled by MybA) were involved in the regulation of nitrate metabolism. The analysis of the transcriptome data by KEGG using the Fungifun browser (https://sbi.hki-jena.de/FungiFun/FungiFun.cgi) showed that the most significantly down regulated pathway was the pyruvate metabolism. Accordingly, the production of acetyl-coA in aerobic respiration to enter the TCA cycle either from acetylcoA-synthetase or pyruvate dehydrogenase was downregulated. Anaerobic degradation of the pyruvate was also downregulated. As a result, the production of energy appeared to be down regulated in the Δ*mybA* mutant.

In agreement with these data, it was shown that the expression of three complexes of the electron transport chain, the succinate dehydrogenase, the NADH dehydrogenase and the cytochrome c oxidase were not affected by the Δ*mybA* deletion. In contrast, all the members of the cytochrome bc1 complex were upregulated in the Δ*mybA* mutant. In this complex, were present the three Rieske proteins annotated in the genome of *A. fumigatus* (AFUA_8G06450, AFUA_3G01160 and AFUA_6G03920) which were among the most highly expressed in the Δ*mybA* mutant strain with GFOLD values of 5.4, 4.1 and 1.6 respectively. Rieske proteins are iron–sulfur cluster binding enzymes that have a high positive reduction potential and they are part of active detoxification systems (Meunier *et al.*, 2013). Their role in *A. fumigatus* has not been investigated yet but their presence in this complex suggested that the high expression of the cytochrome bc1 complex may be more due to a detoxifying function to counteract the

ROS stress rather than a role in the respiratory chain associated with the production in ATP by oxidative phosphorylation. These results suggested that the production of ATP is altered in the Δ*mybA* mutant and that an imbalance in the mitochondrial energy metabolism may play a major role for the loss of conidial dormancy.

Experimental procedures

Construction of strains used in this study

The *A. fumigatus* strain CEA17_Δ*akuB*^{KU80} with improved homologous recombination efficiency (da Silva Ferreira *et al.*, 2006), was used as the recipient strain for *mybA*, *wetA and cspA* gene deletion (Supporting Information Figs. S3, S16 and S17). *A. fumigatus* mutants Δ*abaA*, Δ*brlA*, Δ*velC*, Δ*velB*, Δ*veA* and Δ*vosA*, and their parental strain Af293 were constructed previously (Ni and Yu, 2007; Tao and Yu, 2011; Park *et al.*, 2012a, 2012b). All strains are shown in Supporting Information Table S3. Primers used for the construction of all mutants are listed in Supporting Information Table S4. All DNA construct were amplified by PCR with Phusion enzyme (Thermo Fisher) with a Tm of 65°C.

Construction of mutants

Construction of chlorimuron β recombinase cassette. The pyrithiamine resistance was removed from the vector pSK485 (Hartmann *et al.*, 2010) with the BglII enzyme and replaced by the PCR product of chlorimuron-ethyl resistance (amplified from the vector pCB1637; kind gift from Lebrun's lab). The new vector chlorimuron-ethyl-beta recombinase was verified by restriction enzyme analysis (*Nco*I) and DNA sequencing.

Construction of *the* Δ*mybA* deletion mutant and complemented strains. To delete *mybA*, the *hph* cassette conferring resistance to hygromycin was amplified from the pAN7.1 plasmid (Punt and van den Hondel, 1992), and encompassed with 1 kb upstream and downstream flanking sequences of *mybA*. To construct the complemented strain, a DNA fragment containing 1 kb of upstream flanking sequence of *mybA*, the open reading frame of *mybA* gene, *and* 1 kb *mybA* downstream flanking sequence were assembled together with the Geneart kit (Invitrogen). The *mybA* deletion was complemented at the gene locus in virtue of the double crossing-over event. Conidial transformation was performed by electroporation procedure (Lambou *et al.*, 2010). The constructs and the verification of transformants by Southern blot analysis are shown in Supporting Information Fig. S3.

Construction of mybA:sgfp, h2A:mrfp Pom152::mrfp and mybA::3xha fusions. To construct *mybA:sgfp* under the native *mybA* promoter, the partial ORF (including the second intron and C-terminus) (OZG850/853) and 3′ downstream region (OZG853/855) of the *mybA* locus were amplified from the CEA17_Δ*akuB*^{KU80} parental *A. fumigatus* gDNA. These two fragments were fused to *sgfp-hph* cassette (OZG207/856) with oligos OZG851/854 by fusion PCR leading to 6.1 kb linear fragment that was used for transformation into the CEA17_Δ*akuB*^{KU80} parental strain. Homologous replacement of the *mybA* locus by the *mybA:sgfp-hph* fragment was confirmed by the Southern blot (Supporting Information Fig. S2). The functionality of the MybA::sGfp fusion AFGB47 was validated by growing the Δ*mybA*, *mybA::sgfp* and parental strains on MM medium. To visualize the fungal nuclei, the plasmid pOB207 (*h2A:mrfp under native h2A promoter* in *Kpn*I site of pSK379) carrying a Histone 2A fused to a monomeric red fluorescent protein (*h2A::mrfp*) was transformed into AFGB47 leading to AFGB55 strain (*h2A::mrfp-ptrA*; *mybA::sgfp-hph*; Δ*akuB*::*pyrG*) with red nuclei. To construct *pom152::mrfp* fusion under native promoter, partial ORF (OZG1158/1160) and 3′ downstream region (OZGT1161/1163) of *pom152* were amplified from the CEA17_Δ*akuB*^{KU80} parental gDNA. These two fragments were fused to an *mrfp::phleo* (phleomycin) resistance cassette into *Sma*I site of pUC19 by using In-Fusion HD cloning kit (Clontech) which yielded pOB546. Whole fusion fragment containing partial ORF fused to *mrfp::phleo* and 3′ downstream region was amplified from pOB546 with OZG1159/1162 (6466 bp) and transformed into AFGB47, which yielded AFOB1 used for nuclear pore colocalization experiments. *mybA::3xha* (hemagglutinin) under the native *mybA* promoter was also constructed with the same oligos used for Gfp fusion construction by using fusion PCR. Different from Gfp fusion, Only *3xha::hph* fusion cassette was amplified with OZG916/964. Final *mybA:: 3xha* fusion was introduced into CEA17_Δ*akuB*^{KU80} strain which yielded AFOB2.

Construction of tubA, wetA, vosA and velB promoter glucuronidase fusion reporters. To insert all four glucuronidase reporters into endogenous biotin biosynthesis locus (AFUA_6G03660) and disrupting biotin locus, a recipient plasmid pOB537 was constructed. The targeting of all DNA constructs at the Biotin locus during the genome insertion avoid difference in the expression of the constructs due to putative different ectopic insertion between mutants. 5′(OZG1135/1136) and 3′(OZG1139/1140) of *bioDA* ORF was amplified from the parental gDNA (CEA17_Δ*akuB*^{KU80}) and fused to a *gpdA::phleo* cassette (OZG1137/1138) by cloning in *Sma*I site of pUC19 by using In-Fusion HD cloning (Clontech). An artificial *Swa*I site in pOB537 served to clone four fusion constructs. A 1.5 kb region of tubulin gene promoter *tubA* (OZG1141/1152), transcription factors *wetA* (OZG1146/1155), *vosA* (OZG1148/1156), *velB* (OZG1150/1157) were fused to *uidA* gene encoding glucuronidase (OZG1153/1154) and these fusions were cloned in *Swa*I site of pOB537 leading to ^{p}*tubA::uidA* (pOB542), ^{p}*wetA::uidA* (pOB543), ^{p}*vosA::uidA* (pOB544), ^{p}*velB::uidA* (pOB545). Each plasmid was digested with *Pme*I to release reporter cassettes which were used to transform into CEA17_Δ*akuB*^{KU80} recipient strain. Disruption of *bioDA* gene in transformants was confirmed by lack of growth in minimal media without biotin supplemenet (not shown). Growth only took place in the presence of biotin. *mybA* gene was deleted by using *mybA::ptrA* deletion cassette (pyrithiamine) in strains carrying ^{p}*tubA::uidA* (pOB542),

^{p}*wetA::uidA* (pOB543), ^{p}*vosA::uidA* (pOB544), ^{p}*velB::uidA* (pOB545).

Expression of UidA glucuronidase enzyme reporter was assayed in parental vs *mybA* deletion strains. The reporter strains were grown overnight and equal amount of mycelium were disrupted and an equal amount of protein was used for the fluorometric GUS assay (Jefferson *et al*., 1987). The comparison of the quantity of fluorescent MU product by parental and Δ*mybA* strains carrying the same promoter-reporter construct allowed to quantify the level of expression of *wetA vosA* and *velB* in the parental and mutant strain.

Construction of the ΔwetA strain. The Δ*wetA* deletion mutant was constructed in CEA17_Δ*akuB*^{KU80} background using the β-rec/six site-specific recombination system (Hartmann *et al*., 2010) as described in (Muszkieta *et al*., 2014). Although a Δ*wetA* mutant was existing [3], a new one was constructed to have it in the same Δ*akuB*^{KU80} background of the Δ*mybA* mutant. The gene replacement cassette containing the marker module flanked by 5′ and 3′ upstream and downstream regions of the target gene was generated by PCR using primers using primers listed in Supporting Information Table S4. The deletion at the right locus was confirmed by PCR and Southern blot (Supporting Information Fig. S16).

Construction of the Δ*cspA* strain. A Δ*cspA* mutant was constructed in the 1163/CEA17 Δ*akuB*^{KU80} to have the background same as the *mybA* deletion while the mutant previously analyzed by Levdansky *et al*. (2007) was constructed in a Afu293 background.The parental strain CEA17_ΔakuB ^{ku80} was transformed by homologous recombination with a fused gDNA containing the *cspA* 5′ upstream border, the hygromycin cassette and the *cspA* 3′ downstream. Transformants were selected in 150 μg/ml of hygromycin and their gDNA was used to confirm the right and unique insertion in their genome by PCR and Southern blot techniques (Supporting Information Fig. S17).

Growth and conidiation conditions

All the strains were maintained on 2% malt agar slants at 25°C. Conidia were recovered from these slants using 0.05% Tween 20, and filtered through a 40 μm pore size filter (Falcon).

Measure of the conidial hydrophilicity

The conidia from parental and Δ*mybA* strains were harvested in H_2O and kept static for 40 min. The number of conidia in solution was counted. Tween-20 at a final concentration of 0.05%, was added to these suspensions, mixed them well and counted again. The ratio between the number of conidia in H_20 or H_20–0.05% Tween-20 was a marker of the conidial hydrophobicity.

*Analysis of the conidial surface of the Δ*mybA* mutant*

To analyze the proteins present on the conidial surface of Δ*mybA* strain, 1×10^8 conidia were separately harvested from the parental or Δ*mybA* strains and washed twice with water. Then 100 μl of 0.5M NaCl was added and incubated at RT for 2 hs. A 10 minute centrifugation at 10,000 *g* was performed to recover the NaCl supernatant. 40 μl of each supernatant was loaded on a 10% SDS-PAGE followed by Colloidal Coomassie stained (Beauvais *et al*., 2013)

Confocal spinning disc microscopy

The spinning disc microscopy was performed as given in detail (Bayram *et al*., 2012). The fungal strain AFGB55 coexpressing MybA::sGfp and H2A::mRfp fusions and AFOB1 coexpressing MybA::sGfp and Pom152::mRfp fusions (1000 spores) were grown in a 450 μl liquid minimal medium in multi-well borosilicate slides (Nunc) for 16 h at 37°C. Fluorescence of the MybA::sGfp, His2A::mRfp, Pom152::mRfp fusions were observed with an inverted microscope (Axiovert Observer. Z1, Zeiss) by using 488 nm and 561 nm wavelength lasers. For observation of MybA::sGfp and H2A::mRfp in conidiophore heads, AFGB55 was grown on the surface of solid minimal medium for 15–20 h at 37°C and conidiophores were examined under microscope.

Ha (hemagglutinin) and Gfp-pull-downs, trypsin digest, mass spectrometry and data analysis

Fungal strains, parental *A. fumigatus* CEA17_Δ*akuB*^{KU80} and AFOB1 or AFGB47 expressing respectively MybA::3Ha and MybA::Gfp fusion protein under native promoter were grown in 100 ml Sabouraud liquid medium at 37°C for 20 h with shaking 120 r.p.m. Grown fungal mass was filtered through miracloth and washed twice with dH_2O containing 0.96% NaCl, 1 mM PMSF, 1% DMSO. Dried mycelia were ground and pulverized in liquid nitrogen and used for HA and Gfp pull down experiments. For each pull down experiments 2 ml pulverized fungal mycelia were used. 1 ml breaking buffer (B) (150 mM NaCl, 50 mM Tris HCl pH: 7.6, 10% Glycerol, 0.1% NP-40 containing 1 mM DTT and protease inhibitor cocktail (Roche)) was added to each sample and vortexed for a couple of minutes and kept on ice. Vortexed samples were spun down at 13,000 r.p.m at 4°C for 10 min and cell extracts were removed to the new vials. To each vial 20 μl anti-Ha (Thermo Scientific) or anti-Gfp (Chromotek) magnetic beads, which were prewashed with 1 ml breaking buffer, was added and incubated on a rotator for 2 h at 4°C. The vials were placed on a magnetic rack and beads were washed with ice-cold B buffer for three times. The samples were directly tryptically digested on magnetic beads as described earlier (O'Keeffe *et al*., 2014). Peptide mixtures from pull-down experiments were analyzed in a Thermo Scientific Q-Exactive mass spectrometer (Thermo Fisher) connected with a Dionex RSLCnano system. Results of MS were analyzed by using Proteome Discoverer software (Thermo Fisher). Specific enrichment of proteins in association with Ha- or Gfp-tagged MybA was estimated by the number of peptide spectra matches (PSMs include all spectra leading to identification of a peptide for a given protein, even if several spectra correspond to the same peptide) for three-independent purification

replicates (Supporting Information Table S2). These data were represented as a scatter plot with the control PSM in the *x*-axis and the Ha- or Gfp-associated proteins in the *y*-axis. The proteins that are present in similar levels both in the control and in the purified samples showed similar numbers of PSMs (the diagonal region of the scatter plots). Proteins that are specifically enriched are found in the upper, left part of the graph. In each purification, MybA protein was detected with at least 42 unique peptides coming at the top of the list.

Biochemical analysis of the ΔmybA *mutant conidial cell wall*

For rodlet protein extraction, dry conidia (5 mg) of the parental and Δ*mybA* strains were subjected to formic acid (100%) treatment overnight at 4°C. Extracted proteins (5 μg) were loaded on 15% SDS-PAGE and the protein bands were revealed by colloidal Coomassie blue staining. Identity of the RodA protein was confirmed by Western blot using an anti-RodA antibody (Aimanianda *et al*., 2009). Conidial pigment was extracted according to a method slightly modified from Korytowski and Sarna (1990): conidia were incubated overnight in 10% H_2O_2 at 65°C until conidia are fully bleached. The OD at 310 nm was considered. If the OD is not different between the mutant and parental strain, it indicates that the amount of conidial melanin is identical between the mutant and parental strains. Conidial cell wall polysaccharide composition analysis was performed as described before (Muszkieta *et al*., 2014)

Bioinformatic analyses

The *A. fumigatus* genome annotation data was searched for transcription factors at the Fungal Transcription Factor Database (ftfd.snu.ac.kr). Blast analyses were submitted to the NCBI facility at http://blast.ncbi.nlm.nih.gov/Blast.cgi. Domain prediction was done using Prosite found at http://prosite.expasy.org/ and pSORT II at http://psort.hgc.jp/. Secondary metabolite biosynthetic gene cluster were identified with SMURF (http://jcvi.org/smurf/index.php).

Transcriptome analysis

For the RNA-sequencing experiment, the fungus was grown for 7 days on malt agar at 37°C at room temperature. RNA isolation, and mRNA library construction were carried out as described by Gibbons *et al*. (2012). Illumina reads were quality and adapter trimmed using trim galore (https://www.bioinformatics.babraham.ac.uk/projects/trim_galore/) using a quality cut-off of 20 and a minimum length cut-off of 40 bp. Quality trimmed reads were then mapped against the reference *A. fumigatus* Af293 genome using the "sensitive" pre-set parameters in bowtie2 (Langmead and Salzberg, 2012). We identified differentially expressed genes using GFOLD, which was designed for experiments with no biological replicates. This software package assigns reliable statistics for gene expression differences based on the posterior distribution of log fold change (Feng *et al*., 2012 – doi: 10.1093/bioinformatics/bts515). The raw RNA-seq datasets have been assigned the following accession numbers through NCBI's sequence read archive (http://www.ncbi.nlm.nih.gov/sra), Experiment: SRX528544; Myb1_KO: SRR1264806; KU80_ctrol: SRR1264807. Real-time PCR was performed as described by Wong Sak Hoi *et al*. (2011) and the level of expression was expressed as the ratio of $2^{-\Delta\Delta Ct}$ of the target gene compared with the reference EF1α gene (Livak and Schmittgen, 2001). Values given were the mean of at least 3 replicates ± standard error.

Conidial trehalose content measurement

The *Aspergillus* strains were grown on 2% malt for 9 days at room temperature. Conidia were collected in an aqueous 0.05% Tween-20 solution and filtered with a 40 μm cell strainer. They were washed in distilled water three times, to eliminate all putative traces of glucose coming from the malt medium. For each assay, the trehalose content was measured by two earlier described methods (d'Enfert and Fontaine, 1997; Park *et al*., 2012a, 2012b). Briefly, 3×10^8 conidia were suspended in 300 μl of H_2O and boiled 20 min. The supernatant was recovered by centrifugation (13,000 r.p.m. for 20 min). Sugars and polyols of each supernatant were separated by liquid chromatography using the SARASEP CAR-H, 300 × 7.8 mm column, at 60°C, using 0.008N H_2SO_4 eluent with a flow rate of 0.6 ml/min in a Dionex system. Components were detected by refractive index detector (Precision Instruments IOTA2) and analyzed with the Chromeleon program. The chemical nature of the peaks was assigned with reference carbohydrates (trehalose, mannitol, glycerol, glucose, arabitol and erythritol). Alternatively, 50 μl of the boiled supernatant was treated with 1.3 μl of trehalase enzyme (3.10^{-6} U, Sigma, T8778–1 UN) in 20 mM of ammonium acetate, pH 5.5 at 37°C for 20 h. Samples were dried on a speed-vac, resuspended in 50 μl of H_2O and glucose released by trehalase was quantified as described above. Glucose was measured as a read-out of the presence of trehalose in the samples which were treated with trehalase. The analysis was performed at least in triplicate.

Conidial viability analysis

For the viability assays, conidia on agar slants or conidial suspensions in water (1.5×10^5 in water) were stored at 4°C or 20°C. Storage at −20°C for 1, 4, 6 and 24 h and at 60°C for 5, 10, 15, 30 min was also tested. The viability of conidia was evaluated in triplicate following serial dilutions and plating them on 2% malt plates

GUS assay

Conidia (2×10^7) were plated on cellophane discs placed on top of 1% yeast extract, 3% glucose and 1% agar medium, for 20 h at 30°C. 160 mg of the biofilm containing conidiating mycelium, was suspended in 300 μl of GEB buffer (50 mM sodium phosphate buffer pH 7.0, 10 mM EDTA, 0.1% N-lauroylsarcosine, 0.1 Triton X-100 and

10 mM β-mercaptoethanol; as described in Jefferson *et al.*, 1987), and were disrupted using 150 µl of 0.5 mm glass beads in Fastprep-24 instrument (MP biomedicals) for 2 min with a speed of 6 M/s. Contents were centrifuged at 13,000 r.p.m. during 30 min was performed and the protein concentration of the supernatant was determined by Bio-Rad protein assay at 592nm. Assay was performed in darkness with 0.5 µg of protein, 25 µl of GEB and 225 µl of GEB+ MUG (4-methyl umbelliferyl β-D glucuronide, Calbiochem) at 37°C with 150 r.p.m. shaking.

After 10 min 100 µl of each sample was mixed with 900 µl of the stop buffer (0.2 M Na_2CO_3) and 200 µl of this mixture was loaded on a flat bottom 96 wells black plate. Fluorescence was measured in the Infinite M200 PRO microplate reader (TECAN) with excitation and emission wavelengths of 365 and 455 nm respectively. The calibration curve was performed with concentration from 10 nM to 10 µM of MU standards (4-methylumbeliferone, Clontech) dissolved in stop buffer. For pictures with the UV lamp, 10 µg of protein of each strain was diluted with 100 µl of GEB buffer and 500 µl of 1 mM MUG dissolved in GEB in a PCR tubes. After 20 min tubes were placed on the UV tray and developed on the Gel doc EZ system (Bio-Rad). Pictures were taken with the Image lab software 4.1. The same experiment was also performed with conidia grown at 25° C with some modifications. Conidia were collected and 1×10^8 of them was suspended in 500 µl of GEB and ground in FastPrep 5 times, each time for 1 min at a speed of 6 M/s. Two controls were performed. The first was performed to check if there is or not any tissue autofluorescence. This control was done with the same amount of the tissue proteins of parental strain but without MUG (substrate). The second control was done to check if solutions of the assay did not have performed any autofluorescence. It contained the stop solution and the GEB buffer in the same concentration utilized for each sample.

Electron microscopy. For transmission electron microscopy (TEM), conidia were fixed overnight with 4% glutaraldehyde prepared in 0.1 M cacodylate buffer (pH 7.2). Following several washes in 0.1 M cacodylate buffer, the samples were post-fixed for 1 h in 2% osmium tetroxide (Merck, Darmstadt, Germany) prepared in 0.1 M cacodylate buffer. Dehydration was done in a graded series of 25%, 50%, 75% and 95% ethanol for 5 min each. Samples were dehydrated for 10 min in 100% ethanol and finally in propylene oxide. The samples were then embedded in Agar Low Viscosity resin (Agar scientific, Gometz La Ville). Ultrathin sections (50–60 nm) were performed with an ultramicrotome « Ultracut UC7 » (Leica Microsystems, Vienna, Austria), stained with uranyl acetate and Reynold's lead citrate, and then observed under a Tecnai-biotwin T12 (FEI company) at 100 kV accelerating voltage. Images were recorded using Eagle camera and TIA software. For melanin observation, conidia were exclusively fixed with 4% glutaraldehyde and embedded as described above. Sections were observed without uranylacetate and lead citrate staining. Melanin was seen as the electron dense outerlayer.

For scanning electron microscopy (SEM), agar pieces from sporulating cultures were placed on cover slips and fixed with 2.5% glutaraldehyde prepared in 0.1 M cacodylate buffer overnight. They were then washed three times for 5 min in 0.2 M cacodylate buffer, post-fixed for 1 h in 1% (w/v) osmium tetroxide prepared in 0.2 M cacodylate buffer and then rinsed with distilled water. Samples were dehydrated in ethanol as described for the TEM, followed by critical-point drying with CO_2. Dried specimens were sputtered with 10 nm gold-palladium using a GATAN Ion Beam Coaterand were examined and photographed with a JEOL JSM 6700F field emission scanning electron microscope operating at 5 kV. Images were acquired with the upper SE detector (SEI).

Quantification of superoxide. Conidia (100 µl of 1.10^5 conidia/ml) of the parental and Δ*mybA* strains were grown in RPMI-pH7 without phenol red (Sigma) at 37°C for 19 h on a sterile covered 96-black well plates. Then 5 uM of MitoSOX- Mitochondrial Superoxide Indicator (Thermo Fisher Scientific) was added and the mixture was incubated 15 min in dark. Fluorescence was measured in an Infinite 200 PRO Fluorescence Microplate Reader (Tecan), using excitation and emission wavelengths of 510 and 580 respectively.

In vivo experiments. Mice were cared for in accordance with Institut Pasteur guidelines in compliance with the European animal welfare regulation. Conidial survival assays in lungs after intranasal inoculation of conidia were carried out as described by Lambou *et al.* (2010). Briefly 5×10^8 conidia were inoculated intranasally to immunocompetent OF1 mice. After 36 h, bronchoalveolar lavage was performed and homogenate containing conidia was plated on 2% malt agar and CFUs were counted. The ratio CFUs at 36h/CFUs and 0h is the indicator of the percentage of conidial killing in the mouse lungs. For infection experiments, male BALB/cJ mice (23–28 g, 8 weeks old, R. Janvier, Le Genest Saint-Isle, France) were used as described earlier (Galiger *et al.*, 2013). Four and one days before infection (D-4; D-1), each mouse received an immunosuppressive regimen by intraperitoneal (ip) injection of 200 µl cyclophosphamide (4 mg/ml). Mice were weighed daily to monitor changes in body weight. Mice were then anesthetized by intramuscular injection of 150 µl of a solution containing 10 µg/ml of ketamine and 10 µg/ml xylazine. Mice were given intra-nasally 5×10^4 conidia inoculum (either the parental or Δ*mybA* or complemented Δ*mybA* strains) in a total volume of 25 µl of either the parental or Δ*mybA* or complemented Δ*mybA* strains. Weight and survival of mice were monitored daily over a period of 15 days post infection.

Statistical analyses

Results were statistically analyzed by ANOVA two-way test with a Bonferroni post-test or by Log-rank (Mantel-Cox) test for mouse survival experiment, using GraphPad Prism 6.0 software (GraphPad Software), with a p value below 0.05 considered as significant. For other experiments run in triplicate, ANOVA one or two ways was performed using the JMP1 software (SAS Institute, Cary, NC, USA)

Acknowlegements

This work was supported by DIM programme from Region Ile de France, Fondation pour la Recherche Médicale and ERA-NET Pathogenomics Antifun, the programme Aspergillus of the consortium Aviesan, the Labex IBEID and the Deutsche Forschungsgemeinschaft (DFG). This publication has emanated from research supported in part by a research grant from Science Foundation Ireland (SFI) under Grant Number 13/CDA/2142 to Ozgur Bayram. Ozlem Sarikaya Bayram is supported by the Irish Research Council (IRC) Postdoctoral Fellowship (GOIPD/2014/178). Quantitative protein mass spectrometry facilities were funded by a competitive award from Science Foundation Ireland (12/RI/2346(3)). We thank Mr Betim Karahoda for MybA pull-downs and data analysis.

Conflict of Interest

The authors declare no conflict of interest

Author Contribution

IV, OSB, JWSH, LM constructed most of the mutants used in this study and characterized the phenotype of these mutants, MCP, AM and JKL performed the EM observations. IM, PC and MB constructed and characterized the cspA mutant. OIG performed the animal experiments. JHY and GB provided key mutants for the study. JG and AR helped in the analysis of the RNA seq data and CS in the interpretation of the proteomic data. VA performed some of the biochemical analysis. Initiated by JPL, this study was co-directed by OB and JPL.

References

Ahmed, Y.L., Gerke, J., Park, H.S., Bayram, Ö., Neumann, P., Ni, M., *et al*. (2013) Fungal *velvet* regulators contain a DNA binding domain reminiscent of NF-κB. *PLoS Biol* **11**: e1001750.

Aimanianda, V., Bayry, J., Bozza, S., Kniemeyer, O., Perruccio, K., Elluru, S.R., *et al*. (2009) Surface hydrophobin prevents immune recognition of airborne fungal spores. *Nature* **460**: 1117–1121.

Aitchison, J.D., and Rout, M.P. (2012) The yeast nuclear pore complex and transport through it. *Genetics* **190**: 855–883.

Al-Bader, N., Vanier, G., Liu, H., Gravelat, F.N., Urb, M., Hoareau, C.M., *et al*. (2010) Role of trehalose biosynthesis in *Aspergillus fumigatus* development, stress response, and virulence. *Infect Immun* **78**: 3007–3018.

Albrecht, D., Guthke, R., Brakhage, A.A., and Kniemeyer, O. (2010) Integrative analysis of the heat shock response in *Aspergillus fumigatus*. *BMC Genomics* **11**: 32.

Arguelles, J.C. (2000) Physiological roles of trehalose in bacteria and yeasts: a comparative analysis. *Arch Microbiol* **174**: 217–224.

Arratia-Quijada, J., Sanchez, O., Scazzocchio, C., and Aguirre, J. (2012) FlbD, a Myb transcription factor of *Aspergillus nidulans*, is uniquely involved in both asexual and sexual differentiation. *Eukaryot Cell* **11**: 1132–1142.

Bayram, O., Bayram, O.S., Ahmed, Y.L., Maruyama, J., Valerius, O., Rizzoli, S.O., *et al*. (2012) The *Aspergillus nidulans* MAPK module AnSte11-Ste50-Ste7-Fus3 controls development and secondary metabolism. *PLoS Genet* **8**: e1002816.

Bayram, O., and Braus, G.H. (2012) Coordination of secondary metabolism and development in fungi: the velvet family of regulatory proteins. *FEMS Microbiol Rev* **36**: 1–24.

Bayram, O., Braus, G.H., Fischer, R., and Rodriguez-Romero, J. (2010) Spotlight on *Aspergillus nidulans* photosensory systems. *Fungal Genet Biol* **47**: 900–908.

Bayram, O., Krappmann, S., Ni, M., Bok, J.W., Helmstaedt, K., Valerius, O., *et al*. (2008) VelB/VeA/LaeA complex coordinates light signal with fungal development and secondary metabolism. *Science* **320**: 1504–1506.

Bayry, J., Beaussart, A., Dufrêne, Y.F., Sharma, M., Bansal, K., Kniemeyer, O., *et al*. (2014) Surface structure characterization of *Aspergillus fumigatus* conidia mutated in the melanin synthesis pathway and their human cellular immune response. *Infect Immun* **82**: 3141–3153.

Beauvais, A., Bozza, S., Kniemeyer, O., Formosa, C., Balloy, V., Henry, C., *et al*. (2013) Deletion of the α-(1–3)-glucan synthase genes induces a restructuring of the conidial cell wall responsible for the avirulence of *Aspergillus fumigatus*. *PLoS Pathog* **9**: e1003716.

Beyhan, S., Gutierrez, M., Voorhies, M., and Sil, A. (2013) A temperature-responsive network links cell shape and virulence traits in a primary fungal pathogen. *PLoS Biol* **11**: e1001614.

d'Enfert, C., and Fontaine, T. (1997) Molecular characterization of the *Aspergillus nidulans treA* gene encoding an acid trehalase required for growth on trehalose. *Mol Microbiol* **24**: 203–216.

Dhingra, S., Andes, D., and Calvo, A.M. (2012) VeA regulates conidiation, gliotoxin production, and protease activity in the opportunistic human pathogen *Aspergillus fumigatus*. *Eukaryot Cell* **11**: 1531–1543.

Do, J.H., Yamaguchi, R., and Miyano, S. (2009) Exploring temporal transcription regulation structure of *Aspergillus fumigatus* in heat shock by state space model. *BMC Genomics* **10**: 306.

Elbein, A.D. (1974) The metabolism of alpha, alpha-trehalose. *Adv Carbohydr Chem Biochem* **30**: 227–256.

Feng, J., Meyer, C.A., Wang, Q., Liu, J.S., Liu, X.S., and Zhang, Y. (2012) GFOLD: a generalized fold change for ranking differentially expressed genes from RNA-seq data. *Bioinformatics* **28**: 2782–2788.

Fillinger, S., Chaveroche, M.K., van Dijck, P., de Vries, R., Ruijter, G., Thevelein, J., *et al*. (2001) Trehalose is required for the acquisition of tolerance to a variety of stresses in the filamentous fungus *Aspergillus nidulans*. *Microbiology* **147**: 1851–1862.

Galiger, C., Brock, M., Jouvion, G., Savers, A., Parlato, M., and Ibrahim-Granet, O. (2013) Assessment of efficacy of antifungals against *Aspergillus fumigatus*: value of real-time bioluminescence imaging. *Antimicrob Agents Chemother* **57**: 3046–3059.

Garay-Arroyo, A., Colmenero-Flores, J.M., Garciarrubio, A., and Covarrubias, A.A. (2000) Highly hydrophilic proteins in prokaryotes and eukaryotes are common during conditions of water deficit. *J Biol Chem* **275**: 5668–5674.

Gastebois, A., Aimanianda, V., Bachellier-Bassi, S., Nesseir, A., Beauvais, A., Schmitt, C., *et al*. (2013) SUN proteins belong to a novel family of β-(1,3)-glucan-modifying enzymes involved in fungal morphogenesis. *J Biol Chem* **288**: 13387–13396.

Gibbons, J.G., Beauvais, A., Beau, R., McGary, K.L., Latge, J.P., and Rokas, A. (2012) Global transcriptome changes underlying colony growth in the opportunistic human pathogen *Aspergillus fumigatus*. *Eukaryot Cell* **11**: 68–78.

Hartmann, T., Dumig, M., Jaber, B.M., Szewczyk, E., Olbermann, P., Morschhauser, J., *et al*. (2010) Validation of a self-excising marker in the human pathogen *Aspergillus fumigatus* by employing the beta-rec/six site-specific recombination system. *Appl Environ Microbiol* **76**: 6313–6317.

Jefferson, R.A., Kavanagh, T.A., and Bevan, M.W. (1987) GUS fusions: beta-glucuronidase as a sensitive and versatile gene fusion marker in higher plants. *EMBO J* **6**: 3901–3907.

Korytowski, W., and Sarna, T. (1990) Bleaching of melanin pigments. Role of copper ions and hydrogen peroxide in autooxidation and photooxidation of synthetic dopa-melanin. *J Biol Chem* **265**: 12410–12416.

Lamarre, C., Sokol, S., Debeaupuis, J.P., Henry, C., Lacroix, C., Glaser, P., *et al*. (2008) Transcriptomic analysis of the exit from dormancy of *Aspergillus fumigatus* conidia. *BMC Genomics* **9**: 417–431.

Lambou, K., Lamarre, C., Beau, R., Dufour, N., and Latge, J.P. (2010) Functional analysis of the superoxide dismutase family in *Aspergillus fumigatus*. *Mol Microbiol* **75**: 910–923.

Langmead, B., and Salzberg, S.L. (2012) Fast gapped-read alignment with Bowtie 2. *Nat Methods* **9**: 357–359.

Levdansky, E., Kashi, O., Sharon, H., Shadkchan, Y., and Osherov, N. (2010) The *Aspergillus fumigatus* cspA gene encoding a repeat-rich cell wall protein is important for normal conidial cell wall architecture and interaction with host cells. *Eukaryot Cell* **9**: 1403–1415.

Levdansky, E., Romano, J., Shadkchan, Y., Sharon, H., Verstrepen, K.J., Fink, G.R., *et al*. (2007) Coding tandem repeats generate diversity in *Aspergillus fumigatus* genes. *Eukaryot Cell* **6**: 1380–1391.

Livak, K.J., and Schmittgen, T.D. (2001) Analysis of relative gene expression data using real-time quantitative PCR and the 2(-delta delta C_T) method. *Methods* **25**: 402–408.

Lopez-Berges, M.S., Schafer, K., Hera, C., and Pietro, A.D. (2014) Combinatorial function of velvet and AreA in transcriptional regulation of nitrate utilization and secondary metabolism. *Fungal Genet Biol* **62**: 78–84.

Lopez-Martinez, G., Rodriguez-Porrata, B., Margalef-Catala, M., and Cordero-Otero, R. (2012) The STF2p hydrophilin from *Saccharomyces cerevisiae* is required for dehydration stress tolerance. *PLoS One* **7**: e33324.

Mah, J.H., and Yu, J.H. (2006) Upstream and downstream regulation of asexual development in *Aspergillus fumigatus*. *Eukaryot Cell* **5**: 1585–1595.

Meunier, B., Fisher, N., Ransac, S., Mazat, J.P., and Brasseur, G. (2013) Respiratory complex III dysfunction in humans and the use of yeast as a model organism to study mitochondrial myopathy and associated diseases. *Biochim Biophys Acta* **1827**: 1346–1361.

Mouyna, I., Aimanianda, V., Hartl, L., Prevost, M.C., Sismeiro, O., Dillies, M.A., *et al*. (2016) GH16 and GH81 family ww.ncbi.nlm.nih.gov/pu *Aspergillus fumigatus* are essential for conidial cell wall morphogenesis. *Cell Microbiol* **18**: 128512–128593.

Muszkieta, L., Aimanianda, V., Mellado, E., Gribaldo, S., Alcazar-Fuoli, L., Szewczyk, E., *et al*. (2014) Deciphering the role of the chitin synthase families 1 and 2 in the *in vivo* and *in vitro* growth of *Aspergillus fumigatus* by multiple gene targeting deletion. *Cell Microbiol* **16**: 1784–1805.

Ni, M., and Yu, J.H. (2007) A novel regulator couples sporogenesis and trehalose biogenesis in *Aspergillus nidulans*. *PLoS One* **2**: e970.

O'Keeffe, G., Hammel, S., Owens, R.A., Keane, T.M., Fitzpatrick, D.A., Jones, G.W., and Doyle, S. (2014) RNA-seq reveals the pan-transcriptomic impact of attenuating the gliotoxin self-protection mechanism in *Aspergillus fumigatus*. *BMC Genomics* **15**: 894.

Park, H.-S., Bayram, O., Braus, G.H., Kim, S.C., and Yu, J.-H. (2012b) Characterization of the *velvet* regulators in *Aspergillus fumigatus*. *Mol Microbiol* **86**: 937–953.

Park, H.S., Ni, M., Jeong, K.C., Kim, Y.H., and Yu, J.H. (2012a) The role, interaction and regulation of the velvet regulator VelB in *Aspergillus nidulans*. *PLoS One* **7**: e45935.

Punt, P.J., and van den Hondel, C.A. (1992) Transformation of filamentous fungi based on hygromycin B and phleomycin resistance markers. *Methods Enzymol* **216**: 447–457.

Puttikamonkul, S., Willger, S.D., Grahl, N., Perfect, J.R., Movahed, N., Bothner, B., *et al*. (2010) Trehalose 6-phosphate phosphatase is required for cell wall integrity and fungal virulence but not trehalose biosynthesis in the human fungal pathogen *Aspergillus fumigatus*. *Mol Microbiol* **77**: 891–911.

da Silva Ferreira, M.E., Kress, M.R., Savoldi, M., Goldman, M.H., Hartl, A., Heinekamp, T., *et al*. (2006) The $akuB^{KU80}$ mutant deficient for nonhomologous end joining is a powerful tool for analyzing pathogenicity in *Aspergillus fumigatus*. *Eukaryot Cell* **5**: 207–211.

Soniat, M., and Chook, Y.M. (2015) Nuclear localization signals for four distinct karyopherin-β nuclear import systems. *Biochem J* **468**: 353–362.

Suzuki, S., Sarikaya Bayram, O., Bayram, O., and Braus, G.H. (2013) conF and conJ contribute to conidia germination and stress response in the filamentous fungus *Aspergillus nidulans*. *Fungal Genet Biol* **56**: 42–53.

Tao, L., and Yu, J.H. (2011) AbaA and WetA govern distinct stages of *Aspergillus fumigatus* development. *Microbiology* **157**: 313–326.

Thevelein, J.M., and Hohmann, S. (1995) Trehalose synthase: guard to the gate of glycolysis in yeast? *Trends Biochem Sci* **20**: 3–10.

Welker, S., Rudolph, B., Frenzel, E., Hagn, F., Liebisch, G., Schmitz, G., *et al*. (2010) Hsp12 is an intrinsically unstructured stress protein that folds upon membrane association and modulates membrane function. *Mol Cell* **39**: 507–520.

Wieser, J., and Adams, T.H. (1995) *flbD* encodes a Myb-like DNA-binding protein that coordinates initiation of *Aspergillus nidulans* conidiophore development. *Genes Dev* **9**: 491–502.

Wong Sak Hoi, J., Beau, R., and Latgé, J.P. (2012) A novel dehydrin-like protein from *Aspergillus fumigatus* regulates freezing tolerance. *Fungal Genet Biol* **49**: 210–216.

Wong Sak Hoi, J., Lamarre, C., Beau, R., Meneau, I., Berepiki, A., Barre, A., *et al*. (2011) A novel family of dehydrin-like proteins is involved in stress response in the human fungal pathogen *Aspergillus fumigatus*. *Mol Biol Cell* **22**: 1896–1906.

Wyatt, T.T., Golovina, E., van Leeuwen, A.R., Hallsworth, J.E., Wosten, H.A., and Dijksterhuis, J. (2014a) A decrease in bulk water and mannitol and accumulation of trehalose and trehalose-based oligosaccharides define a two-stage maturation process towards extreme stress resistance in ascospores of *Neosartorya fischeri* (*Aspergillus fischeri*). *Environ Microbiol* **17**: 383–394.

Wyatt, T.T., van Leeuwen, M.R., Golovina, E.A., Hoekstra, F.A., Kuenstner, E.J., Palumbo, E.A., *et al*. (2014b) Functionality and prevalence of trehalose-based oligosaccharides as novel compatible solutes in ascospores of *Neosartorya fischeri* (*Aspergillus fischeri*) and other fungi. *Environ Microbiol* **17**: 395–411.

Wyatt, T.T., van Leeuwen, M.R., Wosten, H.A., and Dijksterhuis, J. (2014c) Mannitol is essential for the development of stress-resistant ascospores in *Neosartorya fischeri* (*Aspergillus fischeri*). *Fungal Genet Biol* **64**: 11–24.

Xiao, N., Suzuki, K., Nishimiya, Y., Kondo, H., Miura, A., Tsuda, S., *et al*. (2010) Comparison of functional properties of two fungal antifreeze proteins from *Antarctomyces psychrotrophicus* and *Typhula ishikariensis*. *FEBS J* **277**: 394–403.

Yu, J.H. (2010) Regulation of development in *Aspergillus nidulans* and *Aspergillus fumigatus*. *Mycobiology* **38**: 229–237.

Supporting information

Additional supporting information may be found in the online version of this article at the publisher's web-site.